Standardization of research methods employed in assessing the interaction metallic-based nanoparticles and the blood-brain barrier: Present and future perspectives

Aisling M. Ross, David Mc Nulty, Colm O'Dwyer, Andreas M. Grabrucker, Patrick Cronin, John J.E. Mulvihill

PII: S0168-3659(19)30049-5
DOI: https://doi.org/10.1016/j.jconrel.2019.01.022
Reference: COREL 9622

To appear in: *Journal of Controlled Release*

Received date: 16 October 2018
Revised date: 16 January 2019
Accepted date: 17 January 2019

Please cite this article as: Aisling M. Ross, David Mc Nulty, Colm O'Dwyer, Andreas M. Grabrucker, Patrick Cronin, John J.E. Mulvihill , Standardization of research methods employed in assessing the interaction metallic-based nanoparticles and the blood-brain barrier: Present and future perspectives. Corel (2019), https://doi.org/10.1016/j.jconrel.2019.01.022

Standardization of research methods employed in assessing the interaction metallic-based nanoparticles and the blood-brain barrier: present and future perspectives

Aisling M. Ross[a,b], David Mc Nulty[c], Colm O'Dwyer[c,d], Andreas M. Grabrucker[a,e,f], Patrick Cronin[a,g], John J. E. Mulvihill[a,b,f,*] john.mulvihill@ul.ie

[a]Bernal Institute, University of Limerick, Limerick, Ireland

[b]School of Engineering, University of Limerick, Limerick, Ireland

[c]School of Chemistry, University College Cork, Cork, Ireland

[d]Micro-Nano Systems Centre, Tyndall National Institute, Lee Maltings, Cork, Ireland

[e]Department of Biological Sciences, University of Limerick, Limerick, Ireland

[f]Health Research Institute, (HRI), University of Limerick, Limerick, Ireland

[g]School of Natural Sciences, University of Limerick, Limerick, Ireland

[*]Corresponding author at: AD3-027, Analog Devices, University of Limerick, Limerick, Ireland.

Abstract

Treating diseases of the central nervous system (CNS) is complicated by the presence of the blood-brain barrier (BBB), a semipermeable boundary layer protecting the CNS from toxins and homeostatic disruptions. However, this layer also excludes almost 100% of therapeutics, impeding the treatment of CNS diseases. The advent of nanoparticles, in particular metallic-based nanoparticles, presents the potential to overcome this barrier and transport drugs into the CNS. Recent interest in metallic-based nanoparticles has generated an immense array of information pertaining to nanoparticles of different materials, varying sizes, morphologies, and surface properties. Nanoparticles with different physico-chemical properties lead to distinct nanoparticle-host interactions; yet, comprehensive characterization is often not completed. Similarly, *in vivo* testing has involved a mixed evaluation of parameters, including: BBB permeability, integrity, biodistribution, and toxicity. The methods applied to assess these parameters are inconsistent; this complicates the comparison of different nanoparticle-host system responses. A systematic review was conducted to investigate the methods by which metallic-based nanoparticles are characterized and assessed *in vivo*. The introduction of a standardized approach to nanoparticle characterization and *in vivo* testing is crucial if research is to transition to a clinical setting. The approach suggested, herein, is based on equipment and techniques that are accessible and informative to facilitate the routine incorporation of this standardized, informative approach into different research settings. Thorough characterization could lead to improved interpretation of *in vivo* responses which could clarify nanoparticle properties that result in favorable *in vivo* outcomes whilst exposing nanoparticle-specific weaknesses. Only then will researchers successfully identify nanoparticles capable of delivering life-saving therapeutics across the blood-brain barrier.

Keywords: Drug delivery, Central nervous system, Blood-brain barrier, Nanomedicine, Metallic-based nanoparticles, Standardization

1 Introduction

As life expectancies continue to rise throughout the world, there is a steady increase in the number of diagnosed cases of brain disorders such as brain tumors, Alzheimer's disease, Parkinson's disease and Huntington's disease [1-4]. While drugs exist that appear to show potential to treat these neurological disorders during experimental testing, few demonstrate clinical therapeutic success [1, 5, 6]. Only ~8.2% of self-originated drugs for the central nervous system (CNS) successfully transition from phase I clinical trials to clinical approval [7]. The vast majority of these drugs are unsuccessful in progressing through phase II and III clinical trials, where failure is usually the result of drug inefficacy [7]. The ability to deliver drugs to their site of action in the CNS, at clinically significant doses, remains the greatest barrier to effective treatment [1, 5, 6, 8].

The limited penetration of drugs into the CNS is primarily attributed to the highly impermeable nature of the brain's microvascular system [5]. The vessel walls, known as the blood-brain barrier (BBB), consist of a layer of endothelial cells, connected by tight junctions [8, 9] which display increased restrictive properties compared to blood vessels throughout the rest of the body [10, 11]. The primary function of the BBB is to restrict paracellular transport into the CNS [11, 12] with diffusion limited to small, lipophilic molecules [8, 13] and metabolite transport typically confined to transcellular movement through the endothelial cells [8]. In this way, the BBB prevents the passage of many harmful substances, such as toxins and pathogens, into the CNS [9, 14, 15]. We refer the reader to Cardoso et al. (2010) for further information regarding the composition and maintenance of the BBB [16]. However, this barrier poses a significant problem for the treatment of CNS diseases [17] as it also prevents the transport of therapeutics from the systemic circulation to the brain [8, 18]. Almost 100% of large molecule drugs and ~98% of small molecule drugs cannot reach therapeutic levels within the brain [1, 17, 19]. Additionally, endothelial cells possess transport proteins that actively remove many cytotoxic drugs and antibiotics from the brain [12], severely limiting treatment strategies. Again, we refer the reader to Patel *et al.* (2009) and Chen *et al.* (2012) for in-depth reviews of BBB transport routes and strategies that can be employed by new drug delivery technologies to enhance delivery across the BBB [20, 21].

Studies now primarily focus on approaches that can be employed to transport therapeutics into the brain. One method involves intentional, temporary breakdown of the BBB via ultrasound [14, 20, 22, 23], inflammatory mediators [11], vasoactive substances [20, 22], alkylglycerols [20], or osmotic disruption [11, 20, 23]. Unfortunately, these methods can lead to later complications [23] such as the penetration of toxins or pathogens into the CNS, edema formation, or disruption to homeostasis [11]. The natural loss of BBB integrity is also exploited in certain brain tumors, known as the "enhanced permeability and retention effect" [23-26]. Malignant astrocytic gliomas such as glioblastoma, the most common and deadly brain tumor [27], experience loss of BBB integrity at the tumor-BBB interfaces [28, 29] resulting in "leaky" vasculature. This increased permeability could be utilized in treatment strategies, where drugs normally excluded from the brain may now penetrate the compromised BBB [30]. However, this is not an ideal strategy; leaky vasculature is seen primarily in later stages of glioma development [23, 31] or at the tumor core [32] while the BBB remains largely intact at the tumor periphery or adjacent to invading cells [32, 33]. Recently, it has been shown that the use of nanoparticles (NPs) could provide an effective but less invasive approach [34, 35]. Metallic-based NPs, in particular, show promise for drug delivery. Over the last decade there have been a great deal of papers detailing sophisticated shape and size controlled synthesis of metallic-based nanoparticles [36-39]. Inherent valancies enable loading with drugs to treat neurological disorders and functionalization with ligands to enhance delivery across the BBB [8, 14]. Although these nanocarriers appear promising, further work is still needed to improve drug delivery efficiency and to address the non-degradative properties [40] which can lead to toxicity and subsequent failure in clinical trials. The future of nanocarrier-based therapy depends on our ability to quantitatively compare the interaction of these diverse and complex NPs with the BBB.

Currently, NPs in use are frequently poorly or inconsistently characterized [41] and there are no universally accepted guidelines for the *in vivo* testing of NPs [42]. Thus, difficulties arise in comparing the performance of the vast array of synthesized NP and assessing the suitability for clinical applications in CNS drug delivery [43] due to the diverse range of approaches currently utilized to characterize NP properties and analyze *in vivo* effects. This results in the generation of apparently contrasting results from different research groups, that makes interpreting NP related data difficult [42]. This review attempts to compare and contrast the current techniques employed during NP characterization and *in vivo* testing. It aims to determine if there

is the potential to introduce a universal and standardized approach to test prospective NP for future clinical applications, using widely accessible instruments and techniques. The use of a standardized approach to characterize and test NPs *in vivo* will facilitate the creation of profiles for novel NPs. Such profiles could be accessed by researchers and the pharmaceutical industry to select NPs, of precise properties, that are best suited to specific CNS applications, based on the reported *in vivo* effects. Such standardization could lead to the discovery of NPs with the potential to carry live-saving therapeutics into the CNS.

2 Review Methodology

The papers reviewed herein were selected according to the PRISMA systematic review process [44]. Papers were found using three databases: Scopus, Academic Search Complete and Web of Science. The search was last conducted in July 2018 using the search strings detailed below.

- Scopus search string:
  - ((TITLE-ABS-KEY ("blood-brain barrier" OR "blood brain barrier" OR b-bb OR bbb) AND TITLE-ABS-KEY (permeability OR transmigration OR transcytosis OR "drug delivery") AND TITLE-ABS-KEY (nano*)) AND (DOCTYPE (ar)) AND (PUBYEAR < 2018) AND (LIMIT-TO (LANGUAGE , "English"))
- Academic Search Complete search string:
  - ("blood brain barrier" OR "blood brain barrier" OR b-bb OR bbb) AND (permeability OR transmigration OR transcytosis OR "drug delivery") AND nano*
  - Search was completed using the default search fields which searched Article Title, the Abstract, the Subject Headings and Keywords. Search was limited to articles, in English, published before December 2017.
- Web of Science search string:
  - TOPIC: ("blood-brain barrier" OR "blood brain barrier" OR bbb OR b-bb) AND TOPIC: (permeability OR transmigration OR transcytosis OR "drug delivery") AND TOPIC: (nano*)
  - Search was refined by DOCUMENT TYPES: (ARTICLE) AND LANGUAGES: (ENGLISH) TIMESPAN: 1945-2017.

Studies were then screened and excluded if the inclusion criteria of the paper were not satisfied. Only original experimental research was included. Papers were excluded if the paper did not specifically investigate NPs that cross the BBB (e.g. papers concerned with intravascular delivery or intranasal delivery were excluded). Further, papers were excluded if the research did not concern metallic-based nanomaterials or if *in vivo* testing was not conducted. Finally, papers were not included if the method of delivery across the BBB involved intentional disruption to the BBB. Figure 1 contains a summary of the papers identified and excluded during the systematic review.

3 Nanoparticles as carriers for drug delivery

NPs are materials smaller than 100 nm in at least one dimension [45, 46]. At the macroscale most materials are inert, however when the same materials are assessed at the nanoscale there is an addition of extraordinary physico-chemical properties [46, 47]. NPs can be processed in a variety of element types [48], shapes, and sizes for application in a range of products and processes that benefit from the novel physical, thermal, optical, and biological properties [49]. Due to their potential for high stability, high drug loading capabilities, and controllable drug release rates many NPs are currently being considered in an effort to overcome the BBB and deliver drugs into the CNS through drug attachment or encapsulation [6, 17].

Despite the ability to cross the BBB, drug delivery facilitated by NPs can face additional challenges. Uncoated polymeric NPs are often identified and degraded by macrophages in circulation, leading to a reduced circulation time and, hence, decreased delivery to the brain [17, 45]. Similarly, lipophilic NPs display excellent biocompatibility and biodegradation but the hydrophobicity results in high clearance from the body by the reticuloendothelial system [50]. Traditionally, polymeric and liposomal NPs were investigated for drug delivery [51]. However, in the last 5 years, there has been a shift in interest towards different materials for drug delivery [51]. Amongst the materials being investigated are metallic-based NPs [51].

Metallic-based NPs, in contrast to polymeric and liposomal NPs, reportedly tend to be non-degradable and minimal clearance *via* the reticuloendothelial system is reported [40, 45]. This maximizes time in circulation, delaying blood elimination, and hence improving the chances of BBB penetration [52]. Additionally, a primary advantage of metallic-based nanoparticles is the highly sophisticated and controllable synthesis methods being developed [36-39]. These results in materials that can be synthesized to relatively small sizes (sub 10 nm) compared to polymeric NPs which reportedly tend to be in the >100 nm range [53, 54]. As it is well established that only very small molecules are capable of crossing the BBB, the ability to produce NPs in the size range of metallic-based NPs could enhance delivery across the BBB. Further, the multivalancies of metallic-based NPs allow functionalization with multiple ligands for specific tissue or cell targeting, facilitating transport across the BBB [8], in addition to loading with drugs [14]. Moreover, metallic-based materials, such as copper, iron and zinc, are considered to be 'essential metals', required for physiological biochemical processes and thus are typically considered non-toxic [55]. However, it is important to note that imbalances to homeostatic levels can lead to toxic effects [55] and so safety of 'essential' metals for application as NPs should not be assumed and must be carefully evaluated for specific clinical applications. As well as the potential to improve biocompatibility, NPs which have magnetic properties, such as iron based materials, can be used in diagnostics as contrast agents for magnetic resonance imaging (MRI) [52, 56]. While, NPs made from high atomic number metals, such as gold, can be used in x-ray based radiotherapy and imaging techniques due to their tendency to absorb x-rays [57]. Such NPs are being investigated for 'theranostic' applications, whereby NPs can act as drug carriers and imaging contrast agents to diagnose and monitor disease progression [56, 58-60]. This takes advantage of the natural properties of the material, without the need for further functionalisation to achieve theranostic properties, as would be the case with other nanomaterials. Future efforts in NP design should aim to combine delivery and diagnostic properties. There have been attempts to combine a number of materials in a single NP delivery system [14, 61-69] to harness the properties of both materials and improve NP efficacy. Work in mixed systems is likely to continue in coming years with the advancement of NP synthesis and improvement to CNS delivery.

However, to further advance this field and properly understand how NP design impacts CNS delivery and biocompatibility, it is important that NPs are fully and consistently characterized. Differences in the reported *in vivo* effects of apparently similar NPs can be found in literature. Different research groups characterize and report different NP properties and the methods applied for characterization also vary. This can lead to NPs, with seemingly similar properties, eliciting different *in vivo* responses including permeation across the BBB, toxicity and cell damage, or biodistribution. Without thorough and consistent characterization of NPs, elucidation of the relationship between NP characteristics and host-system responses is likely to continue to evade researchers.

3.1 Dispersion medium

Prior to beginning characterization, the NP dispersion medium should be considered. NP physico-chemical and morphological properties are dependent on the media in which they are dispersed [70, 71]. For example, the apparent dimensions of NPs change following administration *in vivo* [9]. Here, liquid properties differ from those of dispersion medium in which they were characterized [9]. After administration, plasma proteins may associate with the NPs, forming a new surface named the 'protein corona' [72, 73]. Both synthetic and acquired proteins/peptides on the surface of the NP effect the biodistribution, targeting efficacy, aggregation and toxicity of NPs. Analysis of NPs with regards to the proteins they associate with *in vivo* may be necessary for the prediction of NP-host system interactions [73]. Both protein/protein and protein/nanomaterial interactions will determine some of the behavior of NPs *in vivo* [73, 74]. To account for this complexity, characterization in physiologically relevant solutions [70] should be utilized to understand the surface composition of NPs *ex vivo*. In this way, anticipated *in vivo* NP characteristics can be linked to specific *in vivo* responses. NPs may then be designed, aiming to either suppress protein adsorption to reduce off-target cell uptake, or promote controlled interaction with specific proteins to increase targeting efficiency.

However, some researchers report that dispersing NPs in solutions that mimic physiological salt concentrations and pH results in the formation of coarse agglomerates [70] and that the application of these agglomerated solutions for studies can lead to results that are not representative of physiological responses [70, 75]. Hence, some research advocates characterization in deionized or distilled water to ensure consistent measurements [76].

What is clear is that differences in medium used for dispersion during characterization can impact the properties quoted in the paper. For example, the zeta potential of hydrophilic, functionalized iron oxide NPs characterized between pH 3.0-10.0 showed a change in zeta potential from 40 mV to approximately -30 mV [77]. Of the literature reviewed herein, a diverse range of dispersion media have been used (outlined in Table S1 in the supplementary file). Additionally, 41.3% of papers reviewed did not specify the dispersion medium used, to the best of the authors' knowledge. Thus, the potential for comparing different NP properties is limited. Hence, standardization of a universally applied dispersion medium could facilitate clarification of the similarities and/or differences in the characteristics of distinct NPs.

3.2 Traditional methods of nanoparticle characterization

NP properties are a determining factor for suitability as CNS drug delivery systems [4, 43]. Therefore, there are a number of NP properties that researchers should endeavor to routinely explore during characterization. For example, NP size can affect the absorption, distribution and excretion of NPs [75] and shape can effect distribution and cellular uptake [4]. While, surface charge can have a significant effect on degree of agglomeration, hydrodynamic size, cellular uptake and translocation [75].

Transmission electron microscopy (TEM) is a commonly employed, high-resolution technique used in the characterization of all types of NPs, including metallic-based NPs. Samples for TEM are typically prepared by adding a drop of the dilute NP solution to a carbon-coated copper grid and allowing evaporation of the solvent. TEM generated image can be used to assess core size [1, 2, 8, 9, 12, 14, 23, 24, 32, 41, 42, 61, 62, 64, 66, 68, 77-122], dispersal [1, 9, 14, 32, 42, 64, 66, 77-80, 82-84, 88, 89, 91-96, 98, 100, 104, 106, 107, 115, 116, 119, 120, 122-124], morphology [9, 32, 41, 42, 61, 66, 68, 79-82, 84, 87, 88, 90, 95, 97-100, 102, 104, 105, 108, 110-132], and agglomeration/aggregation [32, 80, 90, 94, 101, 107, 108, 113, 115, 125, 126, 131-133].

Similarly, DLS is another common NP characterization technique that can be applied to measure zeta potential. For nano-sized materials there is no direct method to analyze the surface charge. Instead, zeta potential is calculated [76, 134]. This is a measure of the electrical potential of the double layer formed at the surface of a NP based on its interaction with the solution in which it is dispersed [76]. It can be utilized as an indication of NP stability in solution [135]. It is most commonly measured by dynamic light scattering (DLS) using laser Doppler velocimetry [1, 18, 23, 26, 32, 41, 42, 64, 66, 77, 78, 80, 82-89, 91, 93-95, 97-99, 101, 102, 104, 108-110, 114, 115, 117-119, 122, 126-129, 131, 133, 136-140]. DLS also has the capacity to assess the hydrodynamic size [1, 12, 14, 18, 24, 26, 32, 41, 42, 68, 71, 77, 78, 80, 82-84, 87-89, 91-93, 99, 101, 102, 104, 107-110, 114, 115, 117-120, 122, 127, 129, 130, 133, 136-143], size distribution profile [1, 2, 92, 99, 101, 102, 107, 108, 117, 118, 124, 126, 128, 129, 131, 132, 143], and polydispersity index [1, 24, 26, 71, 77, 78, 87, 88, 92, 99, 101, 104, 107, 110, 115, 124, 129, 140, 142] of NPs.

TEM and DLS are standard, well-established techniques used to analyze all types of NPs. Despite this, these techniques are not being thoroughly applied for the characterization of metallic-based NPs for CNS applications (see Table S2 in the supplementary file for a list of papers that characterized NPs using TEM and DLS and the properties that were examined). The properties analyzed by TEM and DLS are known to impact NP-host system interactions and, hence, the efficacy and biocompatibility of NPs. Although most papers reviewed conducted some form of characterization using these techniques, none of the papers reviewed analyzed all of the above parameter parameters, to the best of the author's knowledge. A breakdown of the frequency with which the aforementioned properties were investigated can be seen in Figure 2.

However, NP phase is particularly important in situations where more than one phase occurs, such as in the case of iron oxide NPs. X-ray diffraction (XRD) can be used to analyze NP crystal structure/phase [61, 62, 66, 69, 80, 87-89, 94, 96, 98, 101, 113, 118, 120, 122, 125, 126, 144-146], as well as purity [61, 80, 96, 101, 102, 113, 120], surface coating [81, 93], or size [94]. Selected-area electron diffraction (SAED) can also be used to investigate crystallinity [94]. Use of a surface area analyzer (SAA) to analyze the NP surface could also be considered. SAAs can obtain the N_2 adsorption-desorption isotherms, providing information regarding the surface properties of the NPs [42, 78, 87, 98, 102, 118, 120, 126, 131, 144, 145].

In addition to these techniques, a number of other characterization methods can be employed to supplement the information gained from TEM and DLS. Methods such as ultraviolet-visible spectroscopy (UV-vis), fluorescent spectroscopy, x-ray fluorescence, inductively coupled plasma optical emission spectroscopy

(ICP-OES), inductively-coupled plasma mass spectrometry (ICP-MS), Infrared spectroscopy (IR), Fourier Transform Infrared spectroscopy (FTIR), x-ray photoelectron spectroscopy (XPS), electron diffraction (ED), energy dispersive x-ray spectroscopy (EDX), electron energy loss spectroscopy (EELS), Raman spectroscopy [88], and neutron activation analysis (NAA) can also be employed. These techniques are primarily concerned with analyzing parameters such as NP solution concentration [1, 8, 9, 26, 41, 68, 80, 85, 103, 107, 124, 133, 137], agglomeration [9, 101, 106], stability [96], purity [94, 101, 110, 118, 120], phase ratio [101, 102], composition [61, 64, 87, 88, 94, 145], and/or structure [32, 62, 66, 89, 101, 122, 131].

While these techniques provide useful information regarding NP solutions, they do not usually provide direct information pertaining to the NP material properties. Therefore, it is less critical for these approaches to be streamlined in future research. Similarly, numerous techniques can be applied to assess ligand binding; however, this review focuses on characterization of the properties of the NP core, which can directly impact NP-host system interfaces and BBB interactions. The methods used to monitor and evaluate NP conjugation generally vary depending on the properties of the ligands or drugs themselves. [96]

3.3 Alternative and additional approaches to nanoparticle characterization

In addition to the commonly employed techniques, there are a number of alternative and novel characterization techniques that have not been utilized considerably. Scanning electron microscopy (SEM) [42, 62, 69, 98, 127, 131, 145], scanning transmission electron microscopy (STEM) [26], or STEM in conjunction with high angle annular darkfield detection [9] have also been applied to assess particle size distribution [9, 26, 98, 127, 131, 145], NP aspect ratio [26, 127], aggregation [125], and morphology [26, 42, 62, 69, 98, 120] as an alternative to TEM. Atomic force microscopy (AFM) can also be used as an alternative to TEM to analyze NP size [83, 101, 145] and morphology [101], as well as phase differences [101].

Nanoparticle tracking analysis (NTA) has been employed to determine NP size and dispersal [136] or the number of NPs in solution as a measure of NP concentration [41]. This concentration is then expressed as NP/mL rather than the traditional g/mL, whereby 1 g of NP could contain different numbers of NPs for NPs of different sizes [41]. However, this method is not suitable for very small NPs (e.g. 20 nm particles) [41, 136].

Another alternative to TEM, for application in estimating agglomeration *in vivo*, is gel electrophoresis. Guerrero *et al.* (2010) estimated the physiological aggregation of NPs in blood by suspending them in plasma [115]. Gel electrophoresis was then applied to analyze the electrophoretic mobility of the NPs following interaction with the plasma proteins [115].

In the case of magnetic metallic-based NPs, magnetic characterization can be performed using a magnetometer [69, 77, 84, 85, 92, 100]. This can also be applied to examine the aggregation of magnetic NPs [85]. Further, the suitability of magnetic NPs for use as MRI contrast agents can be indicated by evaluating relaxation rates under a magnetic field using nuclear magnetic resonance (NMR) spectroscopy [77, 91] or an MRI [80]. Metallic-based NPs such as iron, iron oxide, cobalt, or nickel [147] are particularly suited for use as MRI contrast agents. However, other NPs can be doped with these metals for tailored NP applications [147]. Understanding the magnetic properties of these NPs will be critical in determining their suitability as contrast agents for CNS theranostic applications.

Another technique that can be used to characterize the magnetic properties and dynamics of metallic-based NPs is electron magnetic resonance (EMS), also known as electron spin resonance (ESR) [46]. This technique can be used to examine the superparamagnetic properties of NP dispersions [46]. It has been found that the magnetic behavior of materials is closely related to size; as size increases EMR signals become less intense [148], further signifying the interesting physico-chemical properties associated with nano-scale materials.

There are several advanced characterization techniques for nano-scale materials, which are not yet commonly used or widely available, but have the potential to strengthen the ability to tailor the physical dimensions of metallic-based NPs for use in drug delivery in future research. Standard TEM imaging enables the structural characterization of NPs post-synthesis, however liquid cell transmission electron microscopy (LCTEM) will allow for *in situ* imaging of NP formation during the synthesis procedure [149]. With nanofabricated liquid cells, it will be possible to image through liquids using TEM with sub-nanometer resolution [150]. Reports on topics investigated with LCTEM include *in situ* NP growth and assembly,

manipulation of NPs and *in situ* lithiation of electrode materials for lithium-ion batteries [151-153]. This technique enables researchers to monitor the NP crystallization process in real time [154]. Techniques such as this can have important implications for real-time feedback for the development of NP synthesis processes that produce NPs with characteristics suitable for CNS drug delivery.

Further expansions of this technique include the development of liquid flow transmission electron microscopy, whereby the TEM has been coupled with a microfluidic cell that will allow the dynamic flow of NPs through a hydrated environment during imaging [155]. The use of this technique combined with 3D, microfluidic cell culture models of the BBB [156-159] could provide an opportunity to characterize the real time response of NPs to physiologically relevant environment *in vitro*. This could offer an alternative to the need to conduct TEM in physiologically relevant solutions (as discussed in section 3.1) with the further advantage of providing information relating to the interaction of NPs with cells, mechanisms of cellular uptake, and permeation. Researchers could then determine the feasibility of continuing further research to *in vivo* models for clinical use.

Additionally, characterization techniques such as *in situ* XRD, when coupled with a heating stage, allow for real-time monitoring of the crystal structure of NPs during the synthesis process and can reveal the influence of heating temperature on the phase and size of the NPs being prepared [160]. The application of advanced structural characterization techniques, such as these, will be a crucial step in the realization of metallic-based NPs with dimensions and morphologies which are "made-to-order" for use in CNS drug delivery applications.

Another *in situ* technique combines *in situ* X-ray absorption near edge structure (XANES) and small-angle X-ray scattering (SAXS). Alone, XANES is used to characterize the structure and electronic properties of NPs [161]. This can include oxidation state, structural symmetry, and relative atomic geometries [161]. Meanwhile, SAXS is a technique commonly employed for structural information of biomolecules and NPs in addition to monitoring dynamic conformational changes [162] and to analyze size distribution, shape and polydispersity index of nanomaterials [163]. It is advantageous in so far as it is capable of analyzing materials in physiological solutions, but it lacks high resolution [162]. However, when the individual techniques are combined, it is possible to generate time-resolved, *in situ*, data on the formation of metallic-based NPs that was previously not accessible with conventional techniques for NP formation [164, 165]. Polte *et al.* (2010) give a fresh and in-depth insight on the mechanism of gold NP formation derived from coupled *in situ* XANES and SAXS evaluation [163].

3.4 Recommendation

TEM and DLS are widely used and standard instruments for the assessment of many different types of NPs, including, but not limited to, metallic-based NPs. Together these techniques provide critical information concerning NP characteristics including core size, hydrodynamic size, size distribution profile, dispersal, morphology, zeta potential, agglomeration and polydispersity index. Variations in any one of these properties could impact the interaction of the NPs with the host system and should be thoroughly investigated prior to *in vivo* experiments. NPs are not routinely fully characterized in a consistently manner [41]. Therefore, it is the recommendation of this review that both TEM and DLS should be applied to measure all of the aforementioned NP properties. It is not sufficient to analyze only a subset of these parameters as each parameter has a unique impact of the host system response and will vary between NPs. Techniques such as XRD should also be considered in situations where the NP may be synthesized in different phases, such as iron oxide.

Additionally, researchers should endeavor to investigate TEM and DLS properties in both deionized water and a physiologically relevant solution such as serum, similar to the testing conducted by Zhang *et al.* (2012) [71]. This will allow researchers to anticipate NP properties that can be expected *in vivo* and enable them to better understand how NP properties change in a physiological environment, and hence, how these changes might impact the host system response. These techniques should be applied, at a minimum, to characterize all NPs prior to *in vivo* testing. Figure 3 contains a summary of the recommended, minimum NP characterization.

For theranostic applications, an understanding of the magnetic properties of NPs should be considered. Techniques such as EMS or NMR can provide important information relating to magnetic properties to assess NP suitability as an MRI contrast agent for CNS disorders.

Supplementary to this, in the future researchers could begin to utilize novel techniques, such as LCTEM, for real-time *in situ* investigations of the NP synthesis process. Such in-line characterization steps can improve the synthesis of NPs of sophisticated sizes and shapes, tailored for CNS applications. The incorporation of this technique with microfluidic devices that model the BBB could also prove to be an interesting development in future NP characterization for CNS drug delivery.

It is crucial that future investigations of nanocarrier-based drug delivery, apply a streamlined methodology for NP characterization. Standardization of a universal methodology, using assessable techniques, to conduct NP characterization could lead to more complete and comparable NP profiles. This can aid in understanding the impact different NP properties have on their suitability for applications in CNS drug delivery.

4 *In vivo* Blood-Brain Barrier Interactions of Nanoparticles

Once NPs have been characterized, *in vivo* testing can be employed to monitor the ability of NPs to cross the BBB, to observe NP distribution throughout CNS and the rest of the body, to assess disruption to BBB integrity, and to test the toxic effects of the NPs. An *in vivo* model is advantageous due to its replication of the physiological conditions that would be experienced in a clinical situation [166]. However, inconsistencies in the methods employed to assess these interactions presents complications when comparing results from different studies to evaluate the suitability of NPs for use in the treatment of CNS disease.

4.1 *In vivo* System

In vivo testing provides invaluable insight into the response of a host system to NPs administration [166]. However, different host systems result in distinct NP-host system interactions [167, 168]. Therefore, when attempting to compare the *in vivo* properties of NPs it is important to consider that different animal models may elicit distinct responses to the administered NPs and not all results will be clinically relevant. Higher primates are generally considered to display responses closer to those experienced in a human subject. However, few situations employ higher primates [169], and rodents, including Sprague−Dawley rats [1, 8, 18, 26, 42, 84, 87, 89, 92, 93, 95, 96, 98, 100, 102, 110, 115, 116, 123, 137, 142, 146, 167, 170-174], Wistar rats [9, 12, 61, 62, 64, 65, 69, 77, 83, 91, 93, 105, 106, 133, 175, 176], or mice [14, 23, 24, 41, 63, 66-68, 71, 77, 80-82, 85, 86, 88-90, 93, 94, 97, 101, 103, 104, 107-109, 111, 112, 114, 119, 124-132, 136, 138-144, 167, 175, 177-181], remain the most commonly used animal models for *in vivo* testing.

The use of the Drosophila melanogaster (fruit-fly) is emerging as a simple and potentially informative *in vivo* model of mammalian systems due to its potential for rapid results, the high conservation of genomic information, and the cellular and developmental mechanisms it shares with higher organisms [2, 118] including, specifically, similar neurophysiology [118]. Additionally, due to its rapid life cycle, the impact of NPs on development and aging can be assessed [2]. The use of this model is likely to increase in years to come due to its advantages over conventional models.

4.2 Important parameters

Animal models can be used to evaluate a number of parameters relating to the interaction of NPs with the BBB to estimate their effectiveness as CNS drug delivery vehicles. One of the most important considerations when assessing the suitability of NPs as drug carriers for the treatment of neurological disorders is the ability of the NP to penetrate the BBB and reach the CNS. Based on the literature reviewed, up to 4% of NPs administered (per gram of tissue) cross the BBB [1, 8, 9, 12, 18, 23, 26, 41, 42, 68, 81, 84, 87-90, 93-95, 102-105, 111, 115, 116, 124, 136, 137, 182], or as high as 17.7% in tumor brains [68, 124, 125, 132, 142]. However, methods utilized to assess this are highly varied (summarized in Table 1), impacting the opportunity to confidently compare the results of different studies. If NPs are not capable of significant traversal of the BBB, the drug payload will not be delivered to the site of action at clinically relevant levels. Despite the importance of determining permeation, although it is examined to some extent in ~86% papers (Figure 4), many papers do not quantify the levels at which NPs cross the BBB.

Once it is verified that NPs can permeate into the brain, it is important to examine the distribution of those NPs within the CNS. NPs within the CNS must be effectively targeted to diseased tissues or cells to be beneficial; incorrect targeting of drug-NP conjugates to the site of action in the CNS could reduce the therapeutic effect or lead to damage of healthy cortical cells. If the CNS distribution profiles of different NPs are identified, researchers could use these profiles to select the NP best suited to the drug delivery requirements of a specific application.

Further to CNS distribution, although functionalization of NPs with BBB or cell targeting ligands can improve the accumulation of NPs in the CNS, a significant portion of NPs remain in systemic circulation or are delivered to systemic organs. The targeting of NPs to systemic organs limits the NPs available for permeation into the CNS, reducing the prospect of the NPs reaching the site of action at therapeutically significant levels. Information regarding the extent to which different NPs are distributed to secondary organs could be leveraged to improve targeting of the NPs to the brain, and away from these organs. This can also minimize side effects that may result from mistargeting of drug-conjugated NPs intended to reach the CNS.

As NPs permeate across the BBB, in some instances, this can result in breakdown of the BBB. In certain cases, the intention is to cause transient, reversible disruption of the BBB to enhance NP permeability [112]. Whether the breakdown is intentional or not, it is important to assess the integrity of the BBB following treatment with NPs. Disruption to BBB integrity during treatment of CNS disorders can allow toxins and pathogens, normally excluded, to enter the brain, lead to disruptions of brain homeostasis or result in secondary side-effects [11]. Disruption to the BBB should be avoided, where possible to prevent these complications as they can be detrimental to patient health. The brain exists in a tightly regulated and controlled environment where disruptions to homeostasis can cause alterations or damage to neurological cells and processes. Cellular or tissue damage, as a result of the presence or accumulation of NPs in the brain, needs to be carefully assessed before consideration for clinical applications.

Finally, systemic toxicological studies are necessary to determine if other adverse effects occur as a result of NP treatment. These harmful effects can be exacerbated by accumulation of NPs in tissues not intended to receive treatment. An understanding of the systemic distribution of NPs, as mentioned above, can assist in evaluating toxicological effects.

Despite significant importance, these parameters are not routinely examined during *in vivo* testing. Often, a paper emphasizes one aspect of NP testing and as such, complete testing is not conducted. In such a study, a thorough investigation into the parameter in question is conducted. However, to consider the NP a success for CNS delivery, favorable outcomes for all the aforementioned parameters are necessary. Figure 4 contains a summary of the number of papers reviewed that examined the parameters deemed to be critical for CNS delivery, to the best of the authors' knowledge.

Further, when these parameters are examined, a variety of techniques are utilized (summarized in Table 1). The variety of techniques used prevents researchers from directly comparing the results of different studies. Section 4.3 contains a discussion of techniques commonly used to assess metallic-based NPs for applications in CNS drug delivery. A number of techniques can be used to assess multiple parameters. As such, the following section has been organized according to technique. Each technique is reviewed in terms of parameters that can be assessed and usefulness for evaluation of NPs for CNS drug-delivery. Only techniques that were deemed to be commonly employed or offer unique insight were included. Other techniques used can be found in Table 1.

4.3 Techniques used *in vivo* testing

4.3.1 Observation

Observation and pathology are primarily applied to evaluate toxicological effects of NPs. Prior to euthanasia, preliminary evaluation of the toxic effects of NPs can be achieved by assessing the subjects' physiological state. This commonly includes monitoring weight [24, 66-68, 86, 93, 95, 98, 106, 114, 116, 124, 138, 142, 175], behavior [66-69, 86, 91, 93, 96, 98, 102, 106, 108, 111, 116, 119, 133, 137, 138, 142, 146], appearance [86, 133], activity [93], respiration [102, 167, 183, 184], or mortality [24, 66, 102, 108, 111, 114, 116, 142]. Measurements can also include body temperature [146, 183], heart rate [167, 184], mean arterial blood pressure [146, 167, 183, 184], arterial pH [167, 183, 184], or blood gases levels [146, 183, 184]. A variety of cognitive tests [86, 93, 94, 119, 137, 146, 172, 181] and motor tests [88, 89, 94, 137, 146, 172] can also be conducted on live animals to assess possible neurological deficits resulting from NP administration.

Researchers primarily use observation to monitor the health of the test subject and avoid unnecessary discomfort or pain resulting from administration of the NPs. However, this is an initial indication of toxicity or health and is not sufficient for full toxicological evaluations. More in-depth and quantitative assessments are required to determine if the NPs are safe for use in a clinical setting.

The fruit-fly is an interesting model that can be used to examine toxicity by monitoring the survival rates and behavior of treated Drosophila at different stages of development (larvae, pupae, and adults) [2]. Biocompatibility can be further assessed by dissecting larvae, which can survive for up to 180 minutes in dissection buffer [2]. Dissected larvae are then exposed to a NP solution and their survival rates are monitored [2]. The use of this animal model in future testing could prove to be an informative model for the study of NPs over the model's lifetime, a prospect that is often not feasible with other animal models.

4.3.2 Imaging

In addition to observation, imaging is another technique that can be applied to live animals. In the case of this *in situ* imaging, fluorescent NP can be visualized in the brain or systemic organs by methods including non-invasive fluorescent imaging [23, 97, 98, 107, 114, 124-126, 128, 130, 132, 138, 142, 175] or invasive fluorescent imaging through a cranial window [109, 127]. Often for fluorescent imaging, NPs are tagged with a fluorescent label including, but not limited to, fluorescein isothiocyanate (FITC), carboxyfluoresceine, cy5.5, rhodamine, or N-[2-(dimethylamino)ethyl]-2-[4-[2-(pyridin-4-yl)-1,3-oxazol-5-yl]phenoxy]acetamide (PDMO). Fluorescent probes, such as fluorescein [18, 71, 102, 143], fluorescently tagged Dextran [127], and horseradish peroxidase [102], can also be used for live assessment of BBB integrity in live microscopy through a cranial window [127]. However, when using *in situ* imaging techniques, it must be noted that it is not possible to remove the circulating blood prior to imaging. Therefore, NPs in circulation may contribute to apparent NP levels in organs, and as such these techniques are not useful to accurately quantify NPs levels in different organs.

For magnetic or gadolinium labelled NPs, live imaging can make use of a gamma camera [113], computed tomography (CT) [68, 79, 82], positron emission tomography combined with CT (PET/CT) [8], MRI [14, 24, 32, 68, 69, 77, 80, 83, 85, 91, 92, 101, 110, 125, 141, 142, 171, 174, 175, 177, 179, 180, 186], or magnetic resonance spectroscopy (MRS) [110]. As well as observing NPs in the brain or different organs, MRS can be utilized to observe metabolic changes in the neurological environment following magnetic NP administration by measuring the relative concentrations of metabolites [110]. Alterations in metabolite levels in the brain can indicate neurotoxicity. Such nanoparticles will be well suited for use in experimental stages, allowing both in situ and ex vivo imaging, and for clinical use as theranostic vehicles for diagnostics and disease management.

Table 1: *In vivo* tests conducted to assess parameters pertaining to the use of NPs in the treatment of brain disorders. (FM = Fluorescent Microscopy, CM = Confocal Microscopy, LM = Light Microscopy, GC = gas chromatography, B = brain, L=liver, S = spleen, K= kidneys, H = Heart, Lu = Lungs, Bl = Blood)

Study	**NP Material**	**Animal Model**	**BBB Permeability**	**CNS Distribution**	**Systemic Distribution**		**BBB Integrity**	**Toxicity and Cellular Damage**	
					Method(s)	**Organ(s)**		**CNS**	**Systemic**
Huang *et al.* [118]	Alumina	Drosophila melanogaster						CM Electro-physiological recordings	
Chen *et al.* [143]	Alumina	C57BL/6 Mice	CM	CM			Fluorescein	CM PCR ATP assay	
Sharma *et al.* [167]	Aluminum Copper Silver	Sprague-Dawley rats C57 BALB mice					Evan's blue Radioiodine IHC TEM Water content Electrolyte levels Cerebral blood flow	Histopathology TEM IHC	Observation
Sharma *et al.* [173]	Aluminum Copper	Sprague-Dawley rats					Evan's blue Radioio	Histopathology TEM	

Study	NP Material	Animal Model	BBB Permeability	CNS Distribution	Systemic Distribution		BBB Integrity	Toxicity and Cellular Damage	
					Method(s)	Organ(s)		CNS	Systemic
	Silver						dine Water Content	IHC	
Kaushik *et al.* [88]	Barium Titanate	C57BL\6 mice	TEM STEM CBED ICP-MS	TEM				Histopathology	Observation Histopathology Hematology
Hardas *et al.* [102]	Ceria	Sprague-Dawley rats	TEM ICP-MS	TEM	TEM ICP-MS	B, L B, L, S, Bl	Fluorescein Horseradish peroxidase TEM	Histopathology ROS Assay	Observation Histopathology
Portioli *et al.* [90]	Ceria	C57BL\6 mice	CM TEM ICP-MS	CM TEM	LM CM TEM SEM-EDX ICP-MS	L, S, K, Lu B, L, S, K, Lu B, L, S L B, L, S		IHC	Histopathology
Heckman *et al.* [89]	Ceria	Sprague-Dawley rats C57BL\6 mice SJl/J mice	TEM ICP-MS	TEM	ICP-MS ICP-MS	Bl B, L, S, K			Observation
Kim *et al.* [67]	Cobalt-Iron Oxide-Silica	ICR mice	CM	CM	CM	B, L, S, K, H, Lu, Testis, Uterus	Evan's blue	Histopathology	Observation Histopathology Hematology
Sharma *et al.* [146]	Copper Silver Titanium Dioxide	Sprague Dawley rats					Evan's blue Radioiodine Water content	Observation Histopathology IHC	Observation Histopathology
Sharma *et al.* [183]	Copper Silver Silica	Sprague Dawley rats					Evans' blue Radioiodine Water content	Histopathology IHC	Observation
Sharma *et al.* [184]	Copper Silver	Foster rats					Evan's blue Radioiodine Water content Electrolyte levels Cerebral blood flow	Histopathology TEM	Observation
Sharma *et al.* [172]	Copper Silver	Sprague-Dawley rats					Evan's blue Radioiodine	Observation Histopathology Fluorescent spectromet	

Study	NP Material	Animal Model	BBB Permeability	CNS Distribution	Systemic Distribution		BBB Integrity	Toxicity and Cellular Damage	
					Method(s)	Organ(s)		CNS	Systemic
								ry	
Prades *et al.* [1]	Gold	Sprague−Dawley rats	NAA	FM TEM	NAA	B, L, S			
Frigell *et al.* [8]	Gold	Sprague−Dawley rats	Gamma counter ICP-MS		PET/CT Gamma counter	Whole Body B, L, S, K, H, Bl, Intestine, Urine			
Gromnicova *et al.* [12]	Gold	Wistar rats	LM TEM ICP-MS	LM TEM ICP-MS	ICP-MS	B, L, K, Lu	Anti-IgG		
Garrido *et al.* [103]	Gold	BALB mice	ICP-MS		ICP-MS	B, L, S, K, H, Lu, Bl, Muscle, Tail			
Hari and Kumpati [104]	Gold	Swiss Albino mice	ICP-OES		ICP-OES	B, L, L, K, Bl, Urine			Histopathology Hematology Urine Analysis Organ Indexing Bone Marrow Micronucleus Test
Dixit *et al*. [107]	Gold	Mice (unspecified breed)	Live imaging FM		FM	B, L, S, K, H, Lu, Skin			
Li *et al.* [108]	Gold	ICR mice					Evan's blue		Observation
Peng *et al.* [109]	Gold	Nude mice BALB/C mice	Live imaging FM	FM	ICP-MS	L, K, S, H, Lu, Bl, Skin, Muscle, Urine			
Yin *et al*. [128]	Gold	Nude mice	Live imaging				Live imaging		
Ruan *et al.* [129]	Gold	Kunming mice	CM TEM	CM TEM	CM	L, S, K, H, Lu		Histopathology	Histopathology
Guerrero *et al.* [115]	Gold	Sprague-Dawley rats	FM NAA	FM	FM NAA	B, L, S, K B, L, S, K, Bl	Evan's blue		
Cabezón *et al*. [140]	Gold	ICR-CD1 mice	TEM	TEM					
Feng *et al.* [124]	Gold	Nude mice	Live imaging FM LM ICP-MS	FM LM	Live imaging FM LM ICP-MS	Whole Body B, L, S, K, H, Lu B, L, S, K, H, Lu, B, Bl, Tumor, Urine			Observation
Jensen *et al.*	Gold	CB17 SCID	Live	Live	ICP-MS	B, L, S,	Evan's	Histopatho	Hematolog

Study	NP Material	Animal Model	BBB Permeability	CNS Distribution	Systemic Distribution		BBB Integrity	Toxicity and Cellular Damage	
					Method(s)	Organ(s)		CNS	Systemic
[142]		mice Sprague−Dawley rats	imaging CM LM MRI ICP-MS	imaging CM LM MRI ICP-MS		K, H, Lu, Bl, Tumor, Stomach, Intestine, Pancreas, Eyes, Olfactory Bulb, Pituitary Gland, Adrenal Gland, Fat, Ovary, Skin & Hair, Tail	blue	logy IHC TUNEL staining	y Observation Histopathology Hematology
Ruan *et al.* [132]	Gold	Kunming mice	Live imaging FM PA imaging ICP-OES	FM PA imaging	Live imaging FM	Whole Body B, L, S, K, H, Lu		Histopathology	Histopathology
Ali *et al.* [119]	Gold	C57BL/6N mice						Observation Histopathology	Observation
Nair *et al.* [23]	Gold	Swiss Albino mice	Live imaging FM ICP-OES						
Schäffler *et al.* [78]	Gold	C57BL/6 mice	CM Gamma counter	CM	CM Gamma counter	B, S, K, Lu, B, L, S, K, H, Lu, Bl, Stomach, Large Intestine, Small Intestine, Pancreas, Uterus, Thymus, Aorta, Fat, Muscle, Tail, Bone, Skin, Carcass (tissue after			

Study	NP Material	Animal Model	BBB Permeability	CNS Distribution	Systemic Distribution		BBB Integrity	Toxicity and Cellular Damage	
					Method(s)	Organ(s)		CNS	Systemic
						organ removal), Head, Urine			
Cheng *et al.* [24]	Gold	Athymic Nude mice C57BL/6 mice	LM CM ICP-MS MRI	LM CM MRI	ICP-MS	B, L, S, K, H, Lu, Bl, Bladder, Urine		Histopathology	Observation Histopathology
Lai *et al.* [25]	Gold	BALB/CAnNCg-Foxn1nu/CrlNarl mice	FM X-ray	FM X-ray					
Gao *et al.* [32]	Gold	Athymic Nude mice	LM MRI SERRS	LM MRI SERRS					
Velasco-Aguirre *et al.* [26]	Gold	Sprague-Dawley rats	NAA	TEM	NAA	B, L			
Clark and Davis [139]	Gold	BALB/C mice	LM	LM					
Talamini *et al.* [41]	Gold	CD-1 mice	ICP-MS		ICP-MS LM Darkfield microscopy	B, L, S, K, Lu, Bl, Urine, Feces L, S Lu			
Yang *et al.* [185]	Gold	Sprague-Dawley rats	TEM	TEM					
Kouri *et al.* [138]	Gold	CD1 mice CD17 SCID mice Sprague-Dawley rats	ICP-MS Live imaging ICP-MS FM	Live imaging FM	ICP-MS	B, L, S, K, H, Lu		Histopathology	Hematology Observation Histopathology Hematology
Cabezón *et al.* [178]	Gold	ICR-CD1 mice	SBF-SEM	SBF-SEM					
Chen *et al.* [86]	Gold	BALB/C mice	TEM ICP-MS CARS	TEM ICP-MS CARS				Observation HPLC	Observation
Sela *et al.* [137]	Gold	Sprague-Dawley rats	ICP-MS	ICP-MS	ICP-MS	B, L, S, K, Bl, Urine, CSF		Observation	Observation
Betzer *et al.* [82]	Gold	BALB/C rice	AAS CT	CT	AAS ICP-OES	B, L, S, K, Bl, Pancreas Bl			
Li *et al.* [81]	Gold	S4880202 rice	ICP-MS						
Wiley *et al.* [136]	Gold	BALB/C rice	LM TEM ICP-MS	LM TEM				TEM	
Shilo *et al.*[79]	Gold	BALB/C rice	CT AAS	CT	AAS	B, L, S, K, Bl, Pancreas			

Study	NP Material	Animal Model	BBB Permeability	CNS Distribution	Systemic Distribution		BBB Integrity	Toxicity and Cellular Damage	
					Method(s)	Organ(s)		CNS	Systemic
Sun *et al.* [68]	Gold-Iron Oxide	Nude rice	ICP-MS MRI	MRI ICP-MS	ICP-MS CT	B, Brain Tumor, Muscle, Flank Tumor Bl			Observation
Wang *et al.* [125]	Lanthanide-based (NaYF4:Yb,Er core)	BALB/C mice	Live imaging FM MRI ICP-MS		Live imaging MRI ICP-MS	Whole Body Whole Body L, S, K, H, Lu, Bl, Tumor		Histopathology	Histopathology
Dan *et al.* [18]	Iron Oxide	Sprague−Dawley rats	Gamma counter		Gamma counter	B, L, S, Lu, Bl	Fluorescein		
Mejías et al. [77]	Iron Oxide	Wistar rats C57BL/6 mice	MRI		MRI Magnetometer	B, L L, S, K			
Peiris *et al.* [130]	Iron Oxide	NIH Athymic Nude mice	Live imaging FM	Live imaging FM					
Imam *et al.* [110]	Iron Oxide	Sprague−Dawley rats	MRI	MRI				MRS IHC	
Wang *et al.* [111]	Iron Oxide	ICR mice	AAS		AAS	B, L, S, K, H, Lu, Bl, Stomach, Small Intestine, Bone Marrow,			Observation
Mao *et al.* [112]	Iron Oxide	ACI mice	LM				LM		
Nadeem *et al.* [113]	Iron Oxide	Rabbits	Live imaging		Live imaging	Whole Body			
Mekawy *et al.* [123]	Iron Oxide	Sprague−Dawley rats	TEM	FM			TEM		
Yang *et al.* [174]	Iron Oxide	Sprague Dawley rats	CM MRI	LM CM MRI					
Cheng *et al.* [101]	Iron Oxide	Tg2576 transgenic mice Mice (unspecified breed)	FM MRI	FM MRI					
Wadghiri *et al.* [180]	Iron Oxide	APP/PS1 transgenic mice C57BL/6J mice	LM MRI	LM MRI					
Zhao *et al.* [100]	Iron Oxide	Sprague-Dawley rats	LM HPLC	LM	LM	B, L, S, Lu		Histopathology	
Mu *et al.* [99]	Iron Oxide	Mice (unspecified breed)	FM		FM Fluorescent spectrometry	B, L, S, K, H Blood			
Ansciaux *et al.* [186]	Iron Oxide	NMRI mice	LM Magnetic NMR	LM	Magnetic NMR	B, L, S, K, Lu, Bl,		Histopathology	Histopathology Hematolog

Study	NP Material	Animal Model	BBB Permeability	CNS Distribution	Systemic Distribution		BBB Integrity	Toxicity and Cellular Damage	
					Method(s)	Organ(s)		CNS	Systemic
		APP/PS1 DE9 transgenic mice	MRI	MRI		Urine			y
Vinzant *et al.* [96]	Iron Oxide	Sprague-Dawley rats	CM	CM					Observation
Maritim *et al.* [187]	Iron Oxide	Fischer 344 rats	LM MRI Magnetic NMR	LM MRI					
Marinescu *et al.* [179]	Iron Oxide	Swiss mice	LM MRI	LM MRI					
Fiandra *et al.* [188]	Iron Oxide	BALD/C mice	FM CM	FM CM	Fluorescent spectrometry	Blood			Histopathology
Kumar *et al.* [141]	Iron Oxide	Nude mice	FM LM MRI	FM LM MRI					
Dhakshinamoorthy *et al.* [94]	Iron Oxide	Swiss Albino mice	AAS				Evan's blue	Observation ROS Assay FTIR Western blot	Observation Hematology
Qiao *et al.* [92]	Iron Oxide	Sprague-Dawley rats	MRI	MRI					
Shevtsov *et al.* [91]	Iron Oxide	Wistar rats	CM MRI	CM MRI					Observation
Sillerud *et al.* [85]	Iron Oxide	APP/PS1 DE9 transgenic mice	MRI	MRI					
Huang *et al.* [84]	Iron Oxide	Sprague-Dawley rats	TEM-EDX ICP-OES	TEM-EDX ICP-OES					
Dilnawaz *et al.* [83]	Iron Oxide	Wistar rats	CM LM TEM MRI HPLC	CM LM TEM MRI	MRI HPLC	B, L, Bl B, L, S, K, H, Lu, Bl			
Le Duc *et al.* [171]	Iron Oxide	Sprague-Dawley rats	MRI	MRI					
André *et al.* [177]	Iron Oxide	TG2576 transgenic mice & APP/PS1 DE9 transgenic mice APP/PS1/Tau transgenic mice	LM CM MRI LM MRI	LM CM MRI LM MRI					
Fu *et al.* [170]	Iron Oxide	Sprague-Dawley rats	LM MRI	LM MRI					
Rosillo-de la Torre *et al.* [62]	Iron Oxide-Silica	Wistar rats	TEM	TEM					
Yan *et al.* [61]	Iron Oxide-Silica	Wistar rats	CM TEM	CM TEM	CM	B, L, S, K, H, Lu			
Yim *et al.* [14]	Iron Oxide-Manganes	BALB/c mice	MRI CM	CM	Gamma counter	B, L, H, Lu, Bl	Evan's blue		

Study	NP Material	Animal Model	BBB Permeability	CNS Distribution	Systemic Distribution		BBB Integrity	Toxicity and Cellular Damage	
					Method(s)	Organ(s)		CNS	Systemic
	e								
Hu *et al.* [80]	Manganese Oxide	Kunming mice	MRI	MRI	MRI	Whole Body, B, L, K			
Barandeh *et al.* [2]	Silica	Drosophila melanogaster	FM CM	CM	FM	Whole Body		IHC TUNEL staining	Observation Dissection
Jampilek *et al.* [105]	Silica	Wistar rats	FM UHPLC-HRMS	FM					
You *et al.* [131]	Silica	Sprague-Dawley rats			LM	L, K, S, H, Lu			Histopathology Hematology
Hu *et al.* [114]	Silica	Nude mice Sprague Dawley rats	Live imaging FM HPLC	Live imaging FM	Live imaging FM HPLC	Whole Body B, L, S, K, H, Lu B, L		Histopathology TUNEL staining	Observation Histopathology
Zhou *et al.* [126]	Silica	Nude mice	Live Imaging FM		Live imaging	Whole Body		Histopathology	
Baghirov *et al.* [127]	Silica	Mouse (unspecified breed)	Live imaging				Live imaging		
Zhang *et al.* [71]	Silica	C57BL/6 Mice			GC	Adipose Tissue	Fluorescein IHC	RNA profile	
Shi *et al.* [175]	Silica	Wistar rats Nude mice	Live imaging FM MRI TEM Fluorescent spectrometry		Live imaging FM TEM Fluorescent spectrometry	Whole body B, L, S, K, H, Lu B, K B, L, S, K, H, Lu			Observation
Bouchoucha *et al.* [144]	Silica	BALB/C mice	CM						
Liu *et al.* [42]	Silica	Sprague-Dawley rats	ICP-OES				Evan's blue Water content	Histopathology IHC ROS Assay	Hematology
You *et al.* [98]	Silica	Sprague-Dawley rats	Live imaging FM Fluorescent spectrometry	FM Fluorescent spectrometry	Live imaging FM Fluorescent spectrometry	Whole Body B, L, S, K, H, Lu, Tumor B, L, S, K, H, Lu, Bl, Tumor		Histopathology	Observation Histopathology Hematology
Liu *et al.*[97]	Silica	Athymic BALB/C mice	Live imaging FM		Live imaging	Whole Body			
Yang *et al.* [93]	Silica	Kunming mice Sprague Dawley rats	TEM ICP-MS CM	TEM				Histopathology	Observation Observation Histopathology

Study	NP Material	Animal Model	BBB Permeability	CNS Distribution	Systemic Distribution		BBB Integrity	Toxicity and Cellular Damage	
					Method(s)	Organ(s)		CNS	Systemic
		Zebrafish							Hematology Organ Indexing
Yang *et al.* [66]	Silica Silica-Gold	ICR mice							Observation Histopathology
Shevtsov *et al.* [69]	Silica-Iron	Wistar rats	CM MRI Magnetic hysteresis	CM MRI	Magnetic hysteresis	L, S, K, H, Lu, Skin, Muscle			Observation
Zhao *et al.* [65]	Silica-Iron Oxide	Wistar rats	CM	CM					
Ku *et al.* [64]	Silica-Iron Oxide	Wistar rats	CM TEM	CM TEM			TEM		
Shim *et al.* [15]	Silica Zinc Oxide	Rats (unspecified breed)	TEM-(EDX)	TEM-(EDX)			Evan's blue	Histopathology	
Garza-Ocañas *et al.* [9]	Silver	Wistar rats	CM TEM/STEM ICP-MS	TEM/STEM-(EDX) CM	ICP-MS TEM/STEM-(EDX)	B, L, S, K, H, Lu B, L, K, H		STEM-EDX	TEM
Kiruba Daniel *et al.* [106]	Silver	Wistar rats	FM UV-vis		FM UV-vis	B, L, S, K, Lu B, L, S, K, Lu, Bl			Observation Hematology Urine Analysis
Aliev *et al.* [176]	Silver	Wistar rats	TEM	TEM			TEM	Histopathology	
Xu *et al.* [95]	Silver	Sprague-Dawley rats	ICP-MS		ICP-MS	B, Bl	RNA profile	Histopathology RNA profile	Observation Hematology
Hadrup *et al.* [133]	Silver	Wistar rats						HPLC	Observation
Disdier *et al.* [182]	Titanium Dioxide	Fischer F344 rats	ICP-MS		ICP-MS	B, L, S, Lu	Atenolol IHC	IHC RNA profile	IHC
Liu *et al.* [87]	Titanium Dioxide	Sprague-Dawley rats	ICP-MS	ICP-MS			Evan's blue Water content	Histopathology IHC	
Li *et al.* [189]	Titanium Dioxide	Kunming mice	ICP-MS		ICP-MS	B, Bl		Histopathology ROS Assay	Observation Histopathology BALF Assay
Lipiński *et al.* [63]	Yttrium Oxide-Terbium	BLAB/C mice	CM Scanning cytometry	CM Scanning cytometry	CM Scanning cytometry	B, L, S, K, Duodenum B, L, S, K, Duodenum			
Xie *et al.* [181]	Zinc Oxide	Swiss mice						Observation Electro-physiological	Observation

Study	NP Material	Animal Model	BBB Permeability	CNS Distribution	Systemic Distribution		BBB Integrity	Toxicity and Cellular Damage	
					Method(s)	Organ(s)		CNS	Systemic
								recordings	
Kura *et al.* [116]	Zinc-Aluminum	Sprague-Dawley rats	AAS		AAS	B, L, S, K, Bl			Observation Histopathology Hematology Organ indexing

Alternatively, following euthanasia, *ex vivo* histopathological examination of major organs can be applied. Mounted organs can be imaged directly or sectioned and imaged at a higher resolution, *ex vivo*. This can generate information about the interaction of the NPs with the brain capillaries, transport mechanisms, post-penetration fate, distribution to systemic organs or CNS/systemic tissue damage, including loss of BBB integrity. *Ex vivo* imaging commonly includes light microscopy [12, 24, 32, 41, 66, 67, 83, 87, 90, 93-95, 102, 104, 112, 114, 124-126, 129, 131, 132, 136, 138, 139, 141, 142, 146, 170, 172, 173, 177, 179, 180, 183, 184, 186-189], TEM [9, 12, 15, 26, 61, 62, 64, 83, 84, 86, 88-90, 93, 95, 102, 123, 129, 136, 140, 167, 170, 173, 175, 176, 184, 185, 190], or STEM [9, 88, 90, 102].

These techniques do not require fluorescent tagging to detect the NP in the tissue. However, iron oxide and gold NPs can be stained *ex vivo* with Prussian blue [83, 100, 101, 123, 130, 141, 170, 174, 177, 179, 180, 186, 187] or silver [12, 24, 41, 124, 136, 138, 139, 142], respectively, to enhance visualization by light microscopy. Light microscopy can be further enhanced through with staining with Mayer's hematoxylin [15, 138, 139, 177] or hematoxylin and eosin staining [24, 25, 41, 42, 66, 67, 87, 88, 90, 93, 95, 112, 114, 116, 125, 126, 129, 132, 136, 141, 142, 146, 167, 172-174, 183, 188, 189], which can indicate structural and morphological changes to the tissue, NP induced disruption to the BBB, or localization of NPs to damaged tissue for treatment.

Meanwhile, fluorescent microscopy [1, 2, 12, 15, 23, 25, 26, 97-99, 101, 105-107, 109, 114, 115, 123-125, 130, 132, 138, 141, 175, 188] or confocal microscopy [2, 9, 14, 24, 61, 63-65, 67, 69, 78, 90, 91, 93, 119, 129, 142-144, 173, 174, 177, 182, 188] [63] can be applied for visualization of fluorescent or fluorescently-labelled NPs in the brain or systemic organs. The presence of fluorescent probes in the brain can also be determined post-sacrifice. The tissues themselves can also be stained using a variety of dyes (Table 2). High resolution images can be analyzed to examine co-localization of fluorescent NPs within counter-stained cells or subcellular locations. This can provide information relating to the uptake and inter- or intracellular fate of the NPs as well as cell or tissue damage.

Table 2: Stains employed to label tissue sections for light, fluorescent or confocal microscopy.

Stain	Labelling	Reference
4',6-diamidino-2-phenylindole (DAPI)	Cell nucleus	[14, 42, 61, 64, 65, 69, 90, 91, 99, 114, 129-132, 141, 175, 188]
Anti-4G8	Amyloid-beta plaque	[101, 177, 180]
Anti-6E10	Amyloid-beta plaque	[101, 177, 180]
Anti-Aquaporin4	Astrocytes	[42]
Anti-brunchpilot (nc82)	Neural Synapses (Drosophila)	[118]
Anti-factor VIII	Endothelial cells	[143]
Anti-glial fibrillary acid protein (GFAP)	Astrocytes	[42, 143, 146, 183]
Anti-lipoprotein receptor-related protein (LRP1)	Glioma cells	[129]
Anti-legumain	Glioma cells	[132]
Anti-low density lipoprotein receptor related Protein 1 (anti-LRP1)	Endosomes	[129]

Anti-lysosomal-associated membrane protein 1 (anti-LAMP1)	Cell vesicles	[140]
Anti-neuronal specific nuclear protein (anti-NeuN)	Neuronal cells	[14, 61, 64, 65, 67, 96]
Anti-platelet endothelial cell adhesion molecule (also referred to as anti-cluster of differentiation 31) (anti-CD31)	Endothelial cells	[99, 130, 142, 188]
Anti-synaptophysin	Neuronal Synapses	[182]
Fluoro-Jade B	Neuronal Degeneration	[119, 170]
GP120	Golgi apparatus	[2]
Hematoxylin & Eosin	Cell cytoplasm & cell nucleus	[24, 25, 32, 41, 42, 67, 87, 88, 90, 93, 95, 98, 116, 124, 125, 131, 136, 141, 142, 146, 172-174, 183, 188, 189]
Hoechst 33258	Cell nucleus	[63, 105, 109]
Lectin	Endothelial cells	[109, 144]
Lyxol Fast	Axon myelination	[94, 146, 167, 177, 186]
Masson's Trichrome	Cell nucleus & collagen	[186]
Nissl Stain	Neuronal cells	[1, 90, 115, 119, 167, 170, 172, 173, 183, 184, 188]
Nuclear Fast Red	Cell nucleus	[179, 187]
Streptavidin-CY3	Biocytin-loaded neurons	[118]
Toluylene Red	Neural Cells	[100]
Terminal Deoxynucleotidyl Transferase dUTP Nick End Labelling (TUNEL)	Apoptotic cells	[114, 123, 142]

Although imaging techniques provide useful information regarding mechanisms involved in NP permeation and distribution throughout the CNS, as well as offering indications of tissue toxicity, they are less valuable for analyzing degree of permeation. Imaging methods are primarily qualitative or semi-quantitative. As such alternative techniques should be applied when quantitatively assessing the permeation of NPs into the CNS and NP levels in systemic organs.

4.3.3 Spectroscopy and Chromatography

Spectroscopic methods can have useful applications in NP quantification. They can be used to quantify NP levels in the CNS, in different regions of the CNS (distribution), or in systemic organs. The most commonly employed spectroscopic method to quantify BBB permeability in the literature reviewed was ICP-MS [8, 9, 12, 24, 41, 68, 81, 86-90, 93, 95, 102, 124, 125, 136-138, 142, 182]. It was also applied to quantify the distribution of NPs within different regions of the CNS [12, 68, 86, 87, 124, 137, 142], and in systemic organs [9, 12, 24, 41, 68, 89, 90, 102, 103, 109, 125, 137, 138, 142, 182]. The quantification of NPs in different regions of the CNS could indicate the NPs are able to reach the site of action in quantities capable of achieving a therapeutic effect. Meanwhile, NP levels in urine and blood can also be quantified. Urine or feces levels indicate renal clearance of the NPs [24, 41, 109, 124, 137] while blood samples can provide information on NP blood retention and pharmacokinetics [24, 41, 89, 95, 102, 103, 109, 124, 142, 189]. ICP-OES [23, 42, 82, 84, 103, 104, 132] or atomic absorption spectroscopy (AAS) [79, 82, 94, 111, 116] have been similarly applied to measure the permeation of NPs into the brain [23, 42, 79, 82, 84, 94, 104, 111, 116, 132], distribution to systemic organs [79, 82, 84, 103, 104, 111, 116] or blood and urine levels [79, 82, 104, 111, 116].

Alternatively, the quantity of NPs in brain tissue or systemic organs can be deduced using NAA which creates a radioactive NP [1, 26, 115]. The brain is first removed and lyophilized, before sealing by friction welding. It is then exposed overnight to a neutron flux to generate a radioactive sample [1]. The γ-rays emitted by the samples can be counted using a germanium detector coupled to a γ -ray spectrometer to quantify NP concentration [1, 115]. NAA and ICP-MS are considered to be the current gold standards for the quantification of gold in tissue samples [1, 26]. NAA is considered more sensitive than ICP-MS, which in turn is more sensitive than AAS [1]. Thus, methods such as NAA or ICP-MS may be preferable for determining NP concentrations in the brain where the NP content is typically relatively low [1, 26].

For fluorescent or fluorescently tagged NPs, UV-vis [106, 131] or fluorescent spectroscopy [98, 99, 175, 179] have been applied to determine relative brain [106, 175], systemic organ [98, 106, 175] or blood [98, 99, 131, 188] concentration of homogenized tissue samples. Fluorescent spectroscopy [42, 94, 172, 189], as well as HPLC [86, 133], are further used in in a number of biochemical assays to determine neurotoxicity Changes in the levels of these neurotransmitters in brain homogenate or blood can indicate deregulation in the brain, which can affect cognition [86, 172] or BBB dysfunction [172].

4.3.4 Albumin Penetration

Fluorescent dyes have significant use in analyzing BBB integrity. Extravasation of Evan's Blue dye is the most commonly applied method to analyze BBB disruption [14, 15, 42, 67, 87, 94, 108, 115, 142, 146, 167, 172, 183, 184]. The principle of Evan's blue penetration is based on binding of the dye to serum albumin [42, 115, 167]. Serum albumin is typically excluded from the brain as it is not capable of crossing the intact BBB. Breakdown of the BBB results in increased permeability of the dye-albumin conjugate into the brain [115, 167]. Although visual confirmation of dye permeation into the brain is most commonly employed, calorimetry can be utilized for quantitative estimation of permeation of the dye-albumin conjugate [172, 183, 184, 191]. Alternatively, brain sections can be incubated with formamide overnight and the supernatant, containing the dye-albumin conjugate, can be analyzed spectrophotometrically to quantify dye concentration [15, 67, 87, 108].

Gamma counters can also be used to analyze BBB integrity following administration of NPs. Radioiodine (^{131}I), a gamma reporter, will bind to albumin and the subsequent radioactivity of brain sections is monitored using a gamma counter [146, 167, 172, 183, 184, 191]. These methods provide a rapid and useful means of qualitatively assessing BBB disruption. The potential for semi-quantitative assessment further highlights the practicality of this technique.

4.3.5 Fluid Homeostasis

To monitor BBB integrity, researchers have also monitored increased water content and edema formation, or disruption to electrolyte levels [167]. Water content, and hence, brain edema formation, are determined by comparing the wet weight of the brain to the dry weight [42, 87, 146, 167, 183]. Sharma *et al.* considered a 1% increase in water content indicative of edema formation [167, 183]. Similarly, electrolyte content in the brain can also be disrupted as BBB permeability increases and during brain edema formation [167]. Sharma *et al.* (2009) found that brain edema formation correlated well with permeation of Evan's blue dye [167] and that in situations with increased BBB permeability and edema formation, potassium content decreased and sodium content increased [167, 168].

4.3.6 Hematology

Further to BBB damage, hematological studies can be employed to analyze blood serum chemistry as an indication of toxicological reactions [104]. Blood analysis typically includes quantifying complete blood cell and serum biochemical levels [42, 67, 93, 104, 138, 142] to indicate general animal health. Changes in the levels of inflammatory cytokines, such as chemokines, interleukins, interferons, and tumor necrosis factor, can also be investigated to reveal an immune response resulting from the administration of the NPs [95, 138, 142, 182]. Levels of these inflammatory markers in the brain directly can also be measured as an indication of neurotoxicity [182].

Further biochemical analysis of blood can also specifically detect hepatic marker enzymes and nephrotoxicity markers, which indicate liver injury and necrosis or kidney damage, respectively [104]. These markers can include aspartate aminotransferase [67, 88, 93, 98, 104, 116, 131, 138, 142], alanine transferase [67, 88, 93, 104, 116, 138, 142, 186], alkaline phosphatase [88, 93, 104, 106, 116, 138, 142], gamma-glutamyltransferase [116], urea or blood urea nitrogen [67, 88, 93, 104, 106, 116, 131, 138, 142], uric acid [98, 104, 131], or creatinine [67, 88, 93, 104, 106, 116, 138, 142, 186]. Other biochemical markers include Na^+/K^+ ATPase activity which is an indicator of cell membrane depolarization and interference with cellular activities [106]; or lactate dehydrogenase (LDH) levels which are associated with a wide variety of organ pathologies [67, 94, 98, 131].

Finally, biochemical assays for antioxidants are used to detect oxidative stress by monitoring levels superoxide dismutase [104], catalase [104, 106], nitric oxide [94, 104], glutathione (GTH) [106], or thiobarbituric acid [104]. Lipid peroxidation activity assays [106] or nitrotetrazolium blue reduction assays

[94, 104] can also be used to monitor reactive oxygen species (ROS) generation. Reactive oxygen species can be generated as a result of oxidative stress and result in cellular damage [104].

4.3.7 Immunohistochemistry

IHC is another technique used to monitor toxicological response. To assess loss of BBB integrity, antibody based staining for immunoglobulin G (IgG) [12, 174], albumin [167], claudin-5 [71, 143, 182], occludin [71, 143], vonWillibrand Factor [182], or actin [71] have been applied. IgG, similar to albumin, is normally excluded from the brain [12]. Testing of brain tissue with anti-IgG can reveal the permeation of IgG into the brain due to disruption of the BBB [12]. The application of anti-claudin-5, anti-occludin and anti-actin will stain the endothelial cells of the BBB. Changes in the expression patterns of these proteins can indicate damage to brain microvessels and tight junctions caused by NP administration [71].

Neuronal damage is a critical concern when using NPs as CNS drug delivery vehicles. Cysteine string protein (CSP) is a marker of synaptic vesicles and can indicate changes to the axonal transport pathway which can lead to disruptions in the transport of essential nutrients from neuronal cell bodies to the synapses, a crucial process for neuronal survival and growth [2]. Meanwhile, a reduction in axon myelination can be monitored using antibodies against myelin basic protein (MBP) [167, 173]. A reduction in MBP signifies a loss in axon myelination, indicative of neuronal cell damage [167].

Neurodegeneration can also be measured by assessing glial fibrillary acid protein (GFAP) level. GFAP is upregulated in astrocytes, an important cell in neuroprotection [27, 42, 90, 143, 146, 173, 183], when they are activated by damage or stress, a process known as reactive astrogliosis [167]. This is a protective mechanism in the brain; in response to insult or injury, astrocytes will become reactive and form scar tissue to protect the rest of the brain from the identified threat [27]. Aquaporin4 (AQP4) is another astrocytic marker for cell stress that can be analyzed via IHC. AQP4 is a water channel protein believed to be a marker of BBB permeability and edema formation [42].

A number of proteins can also be labeled to evaluate cell stress in the CNS. Cleaved caspase-3 [94] or ADP ribose polymerase [94] can also be used to stain any cells for cell death or damage. Caspase-3 is involved apoptosis [94], while ADP ribose polymerase is overexpressed in response to cell stress, regulating processes such as DNA repair or cell death [94]. The over expression of these proteins in response to NP administration indicates DNA damage caused by ROS [94]. Liu *et al.* (2017a) and Liu *et al.* (2017b) examined oxidative stress and vascular damage using antibodies against phosphylated myosin light chain (MLC) [42, 87]. Phosphorylation of MLC caused by oxidative stress can lead to endothelial cell contraction and opening of the BBB [42].

Increased cell stress can also be monitored by assessing levels of heat shock protein (HSP) [167]. Sharma *et al.* [167] investigated levels of HSP 72 kDa, a HSP implicated in neurodegenerative stress [192]. Its upregulation has been correlated with cell stress pathways resulting from neuropathology [167]. They found there was a correlation between increased HSP expression and BBB breakdown [167]. However, it is unclear whether it is the increased presence of NPs, occurring due to BBB leakage, which leads to increased cell stress or whether it is the breakdown of the BBB itself that causes cell stress. It is also possible that oxidative stress caused by the NPs could lead to free radical release to induce BBB breakdown *via* endothelial cell damage and, hence, a further increase in NP permeability [167, 168]. IHC techniques, when applied thoroughly, provide a beneficial means of assessing the toxicological effects of NPs on different cell types in the CNS.

The list of markers discussed herein is nonexhaustive. Cell toxicity markers should be selected for in-depth analysis, as appropriate, following preliminary assessments.

4.3.8 Future Perspectives

The ability to directly visualize a large number of discrete molecular species inside living cells simultaneously would represent a significant leap forward for the understanding of complex systems and processes such as drug delivery through the BBB. To optimize the application of NPs for drug delivery, it is crucial to understand the nature of the internal barriers of target cells, as well as the spatial and temporal interactions of the drug-coated NPs within the cells. Recently, reported methods have made significant advancements in this regard and are leading the way for a better appreciation of multifarious biological processes. ATP assays can indicate nanoparticle induced damage to metabolic processes [143]. Meanwhile, Chen *et al.* (2016) recently detailed spatially resolved, highly multiplexed RNA profiling in single cells

[193]. The spatial localizations of thousands of RNA species can be determined in single cells through the application of multiplexed error-robust fluorescence *in situ* hybridization (MERFISH).

Nucleic acid assays are also likely to become more popular as a means of analyzing genetic damage. Chromosomal damage can be assessed using the bone marrow micronucleus test [103]. This is used to assess micronucleation of polychromatic erythrocytes (PCEs) resulting from fragmentation of chromosomes during division of erythropoeitic blast cells [103] which is indicative on genetic damage resulting from the interaction of cells with the NPs. Additionally, real-time polymerase chain reaction (PCR) can be used to quantify the messenger-RNA (mRNA) levels to detect alterations in normal cell expression profiles [71, 95, 143, 182]. For example, inflammation can be detected by monitoring levels of pro-inflammatory cytokines such as tumor necrosis factor-α and interleukin-1β, or cell adhesion molecules such as intercellular adhesion molecule-1 and vascular cell adhesion molecule-1 [71], to examine proteins related to cell activity (e.g. synaptophysin for neuronal activity) [182], or to detect the expression of autophagy related genes such as autophagy/beclin 1 regulator 1 or autophagy related protein 3 [143]. Xu *et al.* (2015) used RNA profiling to monitor the expression of tight junction proteins, (occludin, claudin-1, tight junction protein 1, cadherin 1) [95]. Changes in the mRNA levels of these genes could indicate disruptions to normal BBB structure.

Even with recent advancements, it remains challenging to image cellular processes with high sensitivity and selectivity under biological conditions. Fluorescence microscopy remains to be one of the most commonly used methods of imaging biological molecules. However, the depth of information attainable with this method is restricted by a "color barrier" which limits the number of resolvable colors from 2 to 5 (or 7 to 9 if using advanced instrumentation and analysis) [194-197]. This limitation was recently addressed by Wei *et al.* (2016) who reported on super-multiplex vibrational imaging [193]. Stimulated Raman scattering under electronic pre-resonance conditions was used to image target molecules inside living cells with unprecedented levels of vibrational selectivity and sensitivity (down to 250 nanomolar with a time constant of 1 millisecond). Additionally Wei *et al.* (2016) created a palette of triplebond-conjugated near-infrared dyes, each of which displays a single peak in Raman spectral range [193]. The pairing of these dyes with the advanced Raman spectroscopy techniques described, allows for the simultaneous labelling and imaging of up to 24 specific biomolecules. This expansion in the number of resolvable colors for fluorescent imaging from 5 to 24 represents a significant increase in the number of biomolecules that can be imaged at the same time and represents a paradigm shift in the understanding of biological processes which can be achieved through fluorescence microscopy. This advancement holds great potential to increase future understanding of the function and stability of drug-coated NPs during complex biological processes such as cell/tissue penetration and drug-target interactions.

Furthermore, in recent years there has been a great deal of research on the utilization of AFM for the characterization of nanoscale drug delivery systems. Intermittent contact mode AFM has facilitated the investigation of drug delivery systems by recording the elastic or adhesion behavior of particles [198]. Biosensing AFM enables the observation of structural details of molecular assemblies and cell surfaces and can be used to monitor cellular responses to drug-coated NPs [199]. Li *et al.* (2014) recently reported on monitoring of drug actions on cell membrane on the nanoscale using AFM [200]. They demonstrated that the actions of drug-coated NPs on cell membranes, such as topographic changes, elasticity variations and molecular interaction quantification, can be characterized *via* AFM analysis [200].

4.4 Recommendation

Based on the techniques contained in Section 4.3, the authors recommend that, where possible, the following techniques be utilized the measure and assess the aforementioned parameters to empower full *in vivo* characterization.

4.4.1 BBB Permeability

A review of literature that examines NPs for CNS application, 86.2% of research conducted some form of BBB permeation study. The techniques used for permeability assessment were varied with some groups providing only qualitative information while others attempted to quantify NP permeation. In many situations, research groups did not explicitly study the permeation of NPs into the brain. Instead, they observed parameters such as CNS distribution or CNS toxicity. Although, these parameters do indicate that the NPs did traverse the BBB, the quantity at which this was achieved is not examined.

In situ imaging techniques provide useful information pertaining to NP penetration times, without the need to sacrifice multiple animals across various time points. This approach can inform researchers of the kinetics of BBB permeation and its use should be more widely considered in future studies. Typically, during BBB permeation analysis, the animal is sacrificed at a specific time-point. However, it is not always known if this time point will reveal maximum NP levels in the brain and a wide range of permeation times, from ~1 minute to 24 hours have been reported [14, 77, 107, 110, 113, 114, 126, 128, 132, 142].

Although imaging can be semi-quantitative, through the use of image processing software, methods such as ICP-MS or NAA could be more informative. These techniques are highly sensitive, ICP-MS is routinely capable of detecting NPs at concentrations as low as parts per trillion [201]. Hence, they are capable of detecting even minimal penetration of NPs across the BBB.

The standardization of a combination of techniques, such as *in situ* imagining and ICP-MS or NAA, to analyze NP penetration is important in determining the suitability of NPs for CNS applications. However, in addition to the standardization of techniques, the method of sample preparation should also be unified. In many situations, the capillaries and systemic blood are not removed. Capillary-associated NPs as well as blood-borne NPs can be detected during quantification which may not give an accurate reflection of the permeation of NPs into the brain. This will impact the direct comparison of different research. Sela *et al.* reported that the levels of NPs in the brain appeared to be 10 times higher when perfusion was not conducted [137]. Attempts to remove capillaries, by capillary depletion, and systemic blood, through perfusion, should be widely applied.

4.4.2 CNS Distribution

It is important to show, that a NP not only has the potential to cross the BBB into the brain, but also exhibits subsequent, effective distribution within the CNS. Qualitative imaging techniques could provide a valuable insight into the NP distribution and interactions with cells in the CNS. Meanwhile co-localization imaging facilitates visualization of NPs within diseased cells.

The use of NP imagining labels to monitor CNS distribution is useful for both *in vivo* and *ex vivo* imaging. However, the use of such labels could provide false positive results should the labels become detached from the NP surface. As such, researchers should examine the potential *in vivo* detachment of the labels from the surface of the NPs. Observing the leaching of labels from NPs in physiological solutions could indicate the loss of labels from the NP surface [107, 128, 143]. *Ex vivo* labelling of NPs could also be used to observe the presence of NPs in tissue. Co-localization of the signal from the conjugated label and *ex vivo* stain would indicate retention of the label on the NP surface. Once retention is confirmed, these NPs provide a useful avenue to monitor distribution and penetration mechanisms.

The design of theranostic NPs, possessing imaging capabilities in addition to drug delivery capabilities, will be beneficial for qualitative imaging assessments of CNS distribution further to the potential uses in clinical diagnostics and disease progression. As such, standard light or fluorescent imaging strategies can be most useful for qualitative assessment of NP distribution in the CNS. However, dissection of the brain into regions of interested, followed by quantitative assessment, can also be conducted.

4.4.3 Systemic Distribution

Evaluating NP content in secondary organs can further inform researchers of how NPs are taken up by other organs or cleared from the body. The uptake of NPs by secondary organs will reduce NPs available for permeation into the CNS. By reducing secondary organ uptake and increasing circulation time, the ability of the NPs to permeate through the BBB and reach their site of action at therapeutically significant levels could be improved. Techniques such as ICP-MS or NAA can provide quantitative data relating to NP distribution. Quantification of organ levels, relative to the administered dose, can then be compared to brain levels. This can then be leveraged to inform researchers on how different NP properties or ligands and modifications can improve blood half-life and increase BBB permeation.

4.4.4 Blood-Brain Barrier Integrity

Once distribution has been determined, damage induced by the NPs must be considered. This review found that just 25.7% of literature examined the integrity of the BBB following NP administration (Figure 4). Of these studies, BBB integrity is most commonly analyzed using Evan's Blue dye. This method provides simple, visual confirmation of the breakdown of the BBB through the permeation of dye into the brain tissue. For a more in-depth assessment, the tissue can be sectioned and subjected to spectrophotometric fluorescence

intensity testing to obtain a semi-quantitative assessment of disruption to the BBB in different regions of the brain. This semi-quantitative method could be universally applied in future testing to provide a simple but informative measure of the integrity of the BBB following NP administration. Similar to BBB permeation, perfusion should be conducted prior to attempting to quantify Evan's blue permeation.

Although damage to the BBB is not desirable due to the potential for secondary complications, it is worth noting that this might offer a potential opportunity for the delivery of a greater quantity of therapeutics to the brain. As is the case with brain tumors, increased permeation of NPs into the brain is noted compared to healthy brains [68, 124, 132], potentially due to loss of BBB integrity associated with this disease. Thus, following repeated administration, NP levels in the brain could increase with each dose. Notwithstanding, the effect of repeated NP administration warrants further investigation.

4.4.5 CNS Toxicity

To further assess NP-induced damage, microscopic analysis of brain sections can reveal morphological or structural changes to the tissue. Different applications and diseases will target different cells or processes. Thus, the cells and regions examined will vary with each specific application. However, it is also important to note that NPs may result in toxic effects to cells or regions other than the intended target. For this reason, a preliminary microscopic assessment could be important to indicate the regions or cells that require further toxicity examination.

Based on the results of the initial assessment, more cell specific tests can be conducted using techniques such as IHC. IHC analysis of cell specific proteins or process can provide further information on cell toxicity or damage. The list of proteins mentioned in this review is non-exhaustive and research groups should make an informed decision, based on a preliminary assessment, as to the most appropriate proteins or processes to test in each specific situation.

4.4.6 Systemic Toxicity

Finally, systemic toxicity as a result of NP administration must not be ignored. Observation offers a simple indication of systemic toxicity but to obtain informative results, a more in-depth analysis of the toxicological affects can be gleaned through thorough hematology and histopathology. Hematological assessment provides information of systemic response through the analysis of proteins and metabolites in the blood. Alterations to these levels can indicate damage to specific tissues such as the kidneys and liver or the initiation of an immune response. Histopathological assessment can indicate changes to tissue structure and morphology, in particular. These assessments can in turn guide further toxicity studies to explore specific toxicological responses in these tissues.

A summary of the recommended approach for *in vivo* testing of metallic-based NPs for CNS applications is given in Figure 5. The comprehensive inclusion of these tests could help improve the outcomes of clinical trials through the use of a thorough inspection process for NP suitability.

5 Conclusion

NPs show significant promise for the treatment of CNS diseases. The controllable properties of metallic-based NPs offer the potential to traverse the BBB, moving from circulation into the brain. Additionally, the multivalancies and high surface to volume ratio are ideal for functionalization with ligands to enhance CNS targeting or for conjugation with therapeutics. Once these nanocarriers have permeated into the brain, they may deliver lifesaving drugs to the CNS which would otherwise have been excluded.

The wide range of metallic-based NPs available presents challenges in selecting suitable platforms for therapeutic delivery to the CNS. Characteristics such as size, morphology, surface charge and agglomeration play a crucial part in the NP-host system interaction and, particularly, the ability of NPs to cross the BBB. Changes in any one of these NP properties can result in a different host system response. Before attempting to evaluate the NP-host system responses, comprehensive profiling should be conducted. NPs in use are frequently poorly or inconsistently characterized [41]. Techniques such as TEM and DLS are valuable tools in NP characterization, not unique to metallic-based NPs, that provide information pertaining to core size, hydrodynamic size, size distribution profile, dispersal, morphology, zeta potential (as an estimation of surface charge), agglomeration and polydispersity index. Although these techniques are considered 'common-place' in nanoparticle testing, they are not being routinely applied to generate complete NP profiles. An effort by all research groups to utilize these techniques, as a standard, could be a valuable step

towards the unification of NP characterization. Additionally, the dispersal medium used during NP testing can result in differences in the values obtained for NP properties. Characterization in deionized water presents an evaluation of NP properties, independent of exogenous factors, which can be leverage during the synthesis process. However, characterization in a physiologically relevant solution, such as serum, offers the opportunity to assess the potential properties of NPs following *in vivo* administration. It is our recommendation that NP properties be evaluated in both deionized water and in serum using TEM and DLS, at a minimum, as outlined in Figure 6. This will provide critical information pertaining to the properties of various NPs. A thorough understanding of these properties will benefit elucidation of how different properties impact the NP-host system response. This information can be leveraged by future researchers to inform the NP synthesis for the production of NPs with properties capable of overcoming the BBB.

Following this, similar difficulties arise during *in vivo* assessments. *In vivo* models provide vital information in the move towards clinical applications; offering an opportunity to monitor the effects of NPs in a living system. Rodents are the most commonly used animal model due to ease of use and availability although the use of the Drosophila melanogaster may prove to be an interesting and informative model in future studies for evaluation of NP effects on development and lifecycle. The various host systems that can be selected for NP assessment can potentially lead to different *in vivo* responses following NP administration. Thus, it is important to be aware that direct comparisons of NPs, tested in different animal models may not be possible.

Further, the testing carried out by different groups to assess the suitability of NPs for use in CNS treatment applications is varied. Few research groups conduct studies to experimentally investigate and compare the *in vivo* responses of different NPs. Additionally, comparisons of NPs from literature are hindered by the diverse range of parameters evaluated and test methods used. Parameters such as permeability of NPs across the BBB, NP distribution within the CNS and throughout the body, BBB integrity following administration, and toxicological response are all vital in determining NP suitability. A summary of the recommended parameters that should be considered and suggested methods of evaluation are given in Figure 6. Briefly:

- Prior to conducting any *in vivo* analysis, through characterization of the NPs in use should be conducted. This should include characterization in deionized water to facilitate an understanding of the properties of the synthesized NPs. Next the NPs should be characterized in a physiological solution, such as serum, to understand how the properties of the NPs will change once administered. This characterization should include, at a minimum, the use of TEM and DLS to investigate core size, dispersal, morphology, agglomeration/aggregation, zeta potential, hydrodynamic size, size distribution and polydispersity index.
- For *in vivo* analysis, in the case of BBB permeability, initial qualitative assessment using live imaging can be used to select a time point for quantification of NP permeation across the BBB using ICP-MS or NAA.
- A comparison of NP levels, determined using ICP-MS or NAA, in different organs can leveraged for future work to enhance the targeting of NPs to the brain and away from other organs.
- Qualitative assessment of CNS distribution using microscopy and co-localization techniques provides information regarding accumulation of NPs in different regions in the brain and routes by which various cells take up different NPs.
- For measurement of BBB integrity following NP administration, a simple test using Evan's Blue dye can be conducted. Historically, this has been a qualitative assessment, observing permeation of the dye into the brain. However, the brain can further be sectioned and the permeation of the dye can be quantified spectrophotometrically.
- In the case of toxicity testing, systemic and CNS toxicity can be initially assessed qualitatively using histopathology and microscopy, respectively. Hematology can also be employed in systemic toxicity evaluations. These preliminary examinations can provide information to inform more specific testing, such as organ specific toxicity evaluations or cell specific IHC.

Together, these tests offer an indication of the safety and efficacy of different NPs as potential drug delivery vehicles for CNS disease treatment. The recommended NP characterization and testing should be considered a minimum level of testing for all metallic-based NPs. However, the design of novel NPs results in the materials with unique properties that cannot be fully captured by the highlighted test methods. Instead, NP specific testing can be conducted to promote the unique characteristics of the novel nanomaterials and supplement the standardized approach. Together, this will provide information that allows the new NPs to be

compared to existing NPs while still emphasizing the novel material properties. Similarly, in vivo testing can be supplemented with application and NP specific testing.

The use of *in vivo* models, however, can be arduous and costly to conduct. Strict ethical guidelines leave little scope for comparative models and novel NP assessments. Therefore, there is the need to develop an *in vitro* platform which closely mimics *in vivo* BBB properties. Such a model can be used to make valid predictions about BBB crossing and interactions of different NPs. Reproducible models can be used to complete comparative studies of different of NPs to better understand NP-BBB interactions. Microfluidic devices or 'blood-brain barrier-on-a-chip' devices are an interesting future avenue for research in the area of *in vitro* mimetics [158, 159]. As research strives to minimize the requirement for animal studies, these models become increasingly pivotal. Promising results at an *in vitro* stage will identify NPs that should be selected for more in-depth *in vivo* assessments.

In the future, the concerted characterization and *in vivo* testing of NPs may feed into a public database of NP parameters and behaviors. This reference data library would detail NP properties and the resulting *in vivo* responses. Data on NPs will be made accessible to the different users which will boost data sharing and ease comparisons between laboratories, nanocarriers, or applications. Such a database may be accessed during future research to compare the properties and host system responses of novel NPs to existing datasets. This will improve the reproducibility of experimentation and advance the understanding of how different properties impact host system responses. This, in turn, will facilitate the selection of delivery systems best suited to specific clinical applications. As the database expands, for each new therapeutic application, suitable NP carriers may be selected for testing. This will minimize duplication of work, saving time and resources. It could also be leveraged by pharmaceutical companies to advance drug development, decrease the requirement for large scale screening and reduce time-to-market. However, such a database will be most useful when all researchers characterize and test their NPs in a comprehensive and consistent manner. This is crucial to enable comparisons to be made, which is critical to the advancement of this research area.

It is the recommendation of this review that it is necessary to move towards standardized, universally available, and accepted methods for characterizing NPs and assessing their *in vivo* responses. Similar standardization should also be adopted for NPs of other materials, such as polymers and lipids, using techniques suitable for assessing these materials. Without such standardized approaches, comparisons of NPs for use in CNS drug delivery are not possible. This will inhibit progression towards the development of vehicles suitable for the delivery of lifesaving drugs to the CNS.

Funding Source

This work was supported by the Faculty of Science and Engineering PhD Scholarship 2016, University of Limerick, Ireland. The funding source had no involvement in the preparation of this manuscript.

Declaration of interest

None

Figure Captions

Figure 1: Workflow diagram summarizing the sourcing of papers to review and the exclusion criteria used. Based on the PRISMA flow diagram [44].

Figure 2: The percentage of papers reviewed that analyzed different nanoparticle properties using transmission electron microscopy (TEM) and dynamic light scattering (DLS), to the best of the authors' knowledge.

Figure 3: Flow diagram of the suggested minimum NP characterization to be carried out, including medium for NP dispersion, method or instrument to be used, and the parameters to be reported.

Figure 4: The percentage of papers reviewed that analyzed different in vivo parameters during nanoparticle testing, to the best of the authors' knowledge (BBB = blood-brain barrier; CNS = Central Nervous System).

Figure 5: Flow diagram of the suggested minimum parameters to be evaluated during in vivo NP testing and the recommended techniques for evaluating these parameters (NP= nanoparticle; ICP-MS = inductively coupled plasma mass spectroscopy; NAA = neutron activation analysis; IHC = immunohistochemistry).

Figure 6: Summary of the recommended approach to NPs characterization and *in vivo* testing of metallic-based NPs for applications in central nervous system drug delivery (NP = nanoparticle, TEM = transmission electron microscopy, DLS = dynamic light scattering, NAA = neutron activation analysis, ICP-MS = inductively coupled plasma mass spectroscopy).

References

1. Prades, R., et al., *Delivery of gold nanoparticles to the brain by conjugation with a peptide that recognizes the transferrin receptor.* Biomaterials, 2012. **33**(29): p. 7194-7205.
2. Barandeh, F., et al., *Organically modified silica nanoparticles are biocompatible and can be targeted to neurons in vivo.* PloS one, 2012. **7**(1): p. e29424.
3. World Health Organization, *The World health report: 1998: Life in the 21st century: a vision for all: executive summary.* 1998.
4. Saraiva, C., et al., *Nanoparticle-mediated brain drug delivery: overcoming blood–brain barrier to treat neurodegenerative diseases.* Journal of Controlled Release, 2016. **235**: p. 34-47.
5. Soni, S., R.K. Ruhela, and B. Medhi, *Nanomedicine in Central Nervous System (CNS) Disorders: A Present and Future Prospective.* Advanced pharmaceutical bulletin, 2016. **6**(3): p. 319.
6. Sarowar, T. and A.M. Grabrucker, *Nanomedicine and Neurodegenerative Diseases: An Introduction to Pathology and Drug Targets.* Frontiers in Nanomedicine: Nanomedicine and Neurosciences: Advantages, Limitations and Safety Aspects, 2017. **2**: p. 1-60.
7. DiMasi, J.A., et al., *Trends in risks associated with new drug development: success rates for investigational drugs.* Clinical Pharmacology & Therapeutics, 2010. **87**(3): p. 272-277.
8. Frigell, J., et al., *68Ga-labeled gold glyconanoparticles for exploring blood–brain barrier permeability: preparation, biodistribution studies, and improved brain uptake via neuropeptide conjugation.* Journal of the American Chemical Society, 2013. **136**(1): p. 449-457.
9. Garza-Ocañas, L., et al., *Biodistribution and long-term fate of silver nanoparticles functionalized with bovine serum albumin in rats.* Metallomics, 2010. **2**(3): p. 204-210.
10. Abbott, N.J., et al., *Structure and function of the blood–brain barrier.* Neurobiology of disease, 2010. **37**(1): p. 13-25.
11. Abbott, N.J., L. Rönnbäck, and E. Hansson, *Astrocyte-endothelial interactions at the blood-brain barrier.* Nature reviews. Neuroscience, 2006. **7**(1): p. 41.
12. Gromnicova, R., et al., *Localization and mobility of glucose-coated gold nanoparticles within the brain.* Nanomedicine, 2016. **11**(6): p. 617-625.
13. Chen, W., S.C. Mehta, and D.R. Lu, *Selective boron drug delivery to brain tumors for boron neutron capture therapy.* Advanced drug delivery reviews, 1997. **26**(2): p. 231-247.
14. Yim, Y.S., et al., *A facile approach for the delivery of inorganic nanoparticles into the brain by passing through the blood–brain barrier (BBB).* Chemical Communications, 2012. **48**(1): p. 61-63.
15. Shim, K.H., et al., *Assessment of ZnO and SiO2 nanoparticle permeability through and toxicity to the blood–brain barrier using Evans blue and TEM.* International journal of nanomedicine, 2014. **9**(Suppl 2): p. 225.
16. Cardoso, F.L., D. Brites, and M.A. Brito, *Looking at the blood–brain barrier: molecular anatomy and possible investigation approaches.* Brain research reviews, 2010. **64**(2): p. 328-363.
17. Hu, X., et al., *Cholesterol–PEG comodified poly (N-butyl) cyanoacrylate nanoparticles for brain delivery: in vitro and in vivo evaluations.* Drug delivery, 2017. **24**(1): p. 121-132.
18. Dan, M., et al., *Binding, transcytosis and biodistribution of anti-PECAM-1 iron oxide nanoparticles for brain-targeted delivery.* PLoS One, 2013. **8**(11): p. e81051.
19. Bonoiu, A.C., et al., *Nanotechnology approach for drug addiction therapy: gene silencing using delivery of gold nanorod-siRNA nanoplex in dopaminergic neurons.* Proceedings of the National Academy of Sciences, 2009. **106**(14): p. 5546-5550.
20. Patel, M.M., et al., *Getting into the brain.* CNS drugs, 2009. **23**(1): p. 35-58.
21. Chen, Y. and L. Liu, *Modern methods for delivery of drugs across the blood–brain barrier.* Advanced drug delivery reviews, 2012. **64**(7): p. 640-665.
22. Pardridge, W.M., *The blood-brain barrier: bottleneck in brain drug development.* NeuroRx, 2005. **2**(1): p. 3-14.
23. Nair, L., et al., *Blood brain barrier permeable gold nanocluster for targeted brain imaging and therapy: an in vitro and in vivo study.* Journal of Materials Chemistry B, 2017. **5**(42): p. 8314-8321.
24. Cheng, Y., et al., *Blood- brain barrier permeable gold nanoparticles: an efficient delivery platform for enhanced malignant glioma therapy and imaging.* Small, 2014. **10**(24): p. 5137-5150.
25. Lai, S.F., et al., *Gold nanoparticles as multimodality imaging agents for brain gliomas.* Journal of nanobiotechnology, 2015. **13**(1): p. 85.
26. Velasco-Aguirre, C., et al., *Improving gold nanorod delivery to the central nervous system by conjugation to the shuttle Angiopep-2.* Nanomedicine, 2017. **12**(20): p. 2503-2517.

27. Sofroniew, M.V. and H.V. Vinters, *Astrocytes: biology and pathology.* Acta neuropathologica, 2010. **119**(1): p. 7-35.
28. Furnari, F.B., et al., *Malignant astrocytic glioma: genetics, biology, and paths to treatment.* Genes & development, 2007. **21**(21): p. 2683-2710.
29. Lee, S.-W., et al., *Blood-brain barrier interfaces and brain tumors.* Archives of pharmacal research, 2006. **29**(4): p. 265-275.
30. Cuddapah, V.A., et al., *A neurocentric perspective on glioma invasion.* Nature Reviews Neuroscience, 2014. **15**(7): p. 455-465.
31. Dubois, L.G., et al., *Gliomas and the vascular fragility of the blood brain barrier.* Frontiers in cellular neuroscience, 2015. **8**.
32. Gao, X., et al., *Guiding Brain‐Tumor Surgery via Blood–Brain‐Barrier‐Permeable Gold Nanoprobes with Acid‐Triggered MRI/SERRS Signals.* Advanced Materials, 2017. **29**(21): p. 1603917.
33. Agarwal, S., et al., *Delivery of molecularly targeted therapy to malignant glioma, a disease of the whole brain.* Expert reviews in molecular medicine, 2011. **13**.
34. Allen, T.M. and P.R. Cullis, *Drug delivery systems: entering the mainstream.* Science, 2004. **303**(5665): p. 1818-1822.
35. Tibbitt, M.W., J.E. Dahlman, and R. Langer, *Emerging frontiers in drug delivery.* Journal of the American Chemical Society, 2016. **138**(3): p. 704-717.
36. Rosi, N.L. and C.A. Mirkin, *Nanostructures in biodiagnostics.* Chemical reviews, 2005. **105**(4): p. 1547-1562.
37. Jin, R., et al., *Photoinduced conversion of silver nanospheres to nanoprisms.* Science, 2001. **294**(5548): p. 1901-1903.
38. Grzelczak, M., et al., *Shape control in gold nanoparticle synthesis.* Chemical Society Reviews, 2008. **37**(9): p. 1783-1791.
39. Sun, Y. and Y. Xia, *Shape-controlled synthesis of gold and silver nanoparticles.* Science, 2002. **298**(5601): p. 2176-2179.
40. Li, X., et al., *Nano carriers for drug transport across the blood–brain barrier.* Journal of drug targeting, 2017. **25**(1): p. 17-28.
41. Talamini, L., et al., *Influence of size and shape on the anatomical distribution of endotoxin-free gold nanoparticles.* ACS nano, 2017. **11**(6): p. 5519-5529.
42. Liu, X., B. Sui, and J. Sun, *Blood-brain barrier dysfunction induced by silica NPs in vitro and in vivo: involvement of oxidative stress and Rho-kinase/JNK signaling pathways.* Biomaterials, 2017. **121**: p. 64-82.
43. Gioria, S., et al., *Are existing standard methods suitable for the evaluation of nanomedicines: some case studies.* Nanomedicine, 2018. **13**(5): p. 539-554.
44. Moher, D., et al., *Preferred reporting items for systematic reviews and meta-analyses: the PRISMA statement.* Annals of internal medicine, 2009. **151**(4): p. 264-269.
45. Adabi, M., et al., *Biocompatibility and nanostructured materials: applications in nanomedicine.* Artificial cells, nanomedicine, and biotechnology, 2017. **45**(4): p. 833-842.
46. Iravani, S., *EMR of Metallic Nanoparticles*, in *EMR/ESR/EPR Spectroscopy for Characterization of Nanomaterials*. 2017, Springer. p. 79-90.
47. Rimai, D., L. DeMejo, and R. Bowen, *Observations of adhesion‐induced deformations between spheroidal gold particles and conducting substrates.* Journal of Applied Physics, 1989. **65**(2): p. 755-759.
48. Foss Hansen, S., et al., *Categorization framework to aid hazard identification of nanomaterials.* Nanotoxicology, 2007. **1**(3): p. 243-250.
49. Beydoun, D., et al., *Role of nanoparticles in photocatalysis.* Journal of Nanoparticle Research, 1999. **1**(4): p. 439-458.
50. Zhang, L., et al., *Nanoparticles in medicine: therapeutic applications and developments.* Clinical pharmacology & therapeutics, 2008. **83**(5): p. 761-769.
51. Bobo, D., et al., *Nanoparticle-based medicines: a review of FDA-approved materials and clinical trials to date.* Pharmaceutical research, 2016. **33**(10): p. 2373-2387.
52. Cupaioli, F.A., et al., *Engineered nanoparticles. How brain friendly is this new guest?* Progress in neurobiology, 2014. **119**: p. 20-38.
53. Soppimath, K.S., et al., *Biodegradable polymeric nanoparticles as drug delivery devices.* Journal of controlled release, 2001. **70**(1-2): p. 1-20.

54. Kim, K.Y., *Nanotechnology platforms and physiological challenges for cancer therapeutics*, in *Nanomedicine in Cancer*. 2017, Pan Stanford. p. 27-46.
55. Zitka, O., et al., *From amino acids to proteins as targets for metal-based drugs.* Current drug metabolism, 2012. **13**(3): p. 306-320.
56. McNamara, K. and S.A. Tofail, *Nanosystems: the use of nanoalloys, metallic, bimetallic, and magnetic nanoparticles in biomedical applications.* Physical Chemistry Chemical Physics, 2015. **17**(42): p. 27981-27995.
57. Das, S., et al., *Bio-inspired nano tools for neuroscience.* Progress in neurobiology, 2016. **142**: p. 1-22.
58. Ma, Y.-Y., et al., *Molecular Imaging of Cancer with Nanoparticle-Based Theranostic Probes.* Contrast Media & Molecular Imaging, 2017. **2017**.
59. Chen, F., E.B. Ehlerding, and W. Cai, *Theranostic nanoparticles.* Journal of Nuclear Medicine, 2014. **55**(12): p. 1919-1922.
60. Guo, J., et al., *Gold nanoparticles enlighten the future of cancer theranostics.* International Journal of Nanomedicine, 2017. **12**: p. 6131.
61. Yan, F., et al., *Transferrin-conjugated, fluorescein-loaded magnetic nanoparticles for targeted delivery across the blood–brain barrier.* Journal of Materials Science: Materials in Medicine, 2013. **24**(10): p. 2371-2379.
62. Rosillo-de la Torre, A., et al., *Phenytoin carried by silica core iron oxide nanoparticles reduces the expression of pharmacoresistant seizures in rats.* Nanomedicine, 2015. **10**(24): p. 3563-3577.
63. Lipiński, W., et al., *Wide band-gap oxide nanoparticles as potential drug carriers.* Medycyna Weterynaryjna, 2017. **73**(10): p. 657-660.
64. Ku, S., et al., *The blood–brain barrier penetration and distribution of PEGylated fluorescein-doped magnetic silica nanoparticles in rat brain.* Biochemical and biophysical research communications, 2010. **394**(4): p. 871-876.
65. Zhao, H., et al., *Evaluation of Gene-Carrying Ability and Transfection Efficiency of Two Self-Assembled Fluorescein-Doped Magnetic Silica Nanoparticles.* Journal of Nanoscience and Nanotechnology, 2016. **16**(7): p. 7005-7012.
66. Yang, L., et al., *Gold nanoparticle-capped mesoporous silica-based H2O2-responsive controlled release system for Alzheimer's disease treatment.* Acta biomaterialia, 2016. **46**: p. 177-190.
67. Kim, J.S., et al., *Toxicity and tissue distribution of magnetic nanoparticles in mice.* Toxicological Sciences, 2005. **89**(1): p. 338-347.
68. Sun, L., et al., *Theranostic application of mixed gold and superparamagnetic iron oxide nanoparticle micelles in glioblastoma multiforme.* Journal of biomedical nanotechnology, 2016. **12**(2): p. 347-356.
69. Shevtsov, M., et al., *Zero-valent Fe confined mesoporous silica nanocarriers (Fe (0)@ MCM-41) for targeting experimental orthotopic glioma in rats.* Scientific Reports, 2016. **6**.
70. Bihari, P., et al., *Optimized dispersion of nanoparticles for biological in vitro and in vivo studies.* Particle and fibre toxicology, 2008. **5**(1): p. 14.
71. Zhang, B., et al., *Cerebrovascular toxicity of PCB153 is enhanced by binding to silica nanoparticles.* Journal of Neuroimmune Pharmacology, 2012. **7**(4): p. 991-1001.
72. Pederzoli, F., et al., *Protein corona and nanoparticles: how can we investigate on?* Wiley Interdisciplinary Reviews: Nanomedicine and Nanobiotechnology, 2017.
73. Heckman, K.L., et al., *Application of mass spectrometry to characterize localization and efficacy of nanoceria in vivo*, in *Advancements of Mass Spectrometry in Biomedical Research*. 2014, Springer. p. 561-579.
74. Lynch, I., et al., *The nanoparticle–protein complex as a biological entity; a complex fluids and surface science challenge for the 21st century.* Advances in colloid and interface science, 2007. **134**: p. 167-174.
75. Jiang, J., G. Oberdörster, and P. Biswas, *Characterization of size, surface charge, and agglomeration state of nanoparticle dispersions for toxicological studies.* Journal of Nanoparticle Research, 2009. **11**(1): p. 77-89.
76. Honary, S. and F. Zahir, *Effect of zeta potential on the properties of nano-drug delivery systems-a review (Part 1).* Tropical Journal of Pharmaceutical Research, 2013. **12**(2): p. 255-264.
77. Mejías, R., et al., *Liver and brain imaging through dimercaptosuccinic acid-coated iron oxide nanoparticles.* Nanomedicine, 2010. **5**(3): p. 397-408.

78. Schäffler, M., et al., *Blood protein coating of gold nanoparticles as potential tool for organ targeting.* Biomaterials, 2014. **35**(10): p. 3455-3466.
79. Shilo, M., et al., *Transport of nanoparticles through the blood–brain barrier for imaging and therapeutic applications.* Nanoscale, 2014. **6**(4): p. 2146-2152.
80. Hu, X., et al., *Water-soluble and biocompatible MnO@ PVP nanoparticles for MR imaging in vitro and in vivo.* Journal of biomedical nanotechnology, 2013. **9**(6): p. 976-984.
81. Li, M., et al., *Using Multifunctional Peptide Conjugated Au Nanorods for Monitoring β-amyloid Aggregation and Chemo-Photothermal Treatment of Alzheimer's Disease.* Theranostics, 2017. **7**(12): p. 2996.
82. Betzer, O., et al., *The effect of nanoparticle size on the ability to cross the blood–brain barrier: an in vivo study.* Nanomedicine, 2017. **12**(13): p. 1533-1546.
83. Dilnawaz, F., et al., *The transport of non-surfactant based paclitaxel loaded magnetic nanoparticles across the blood brain barrier in a rat model.* Biomaterials, 2012. **33**(10): p. 2936-2951.
84. Huang, Y., et al., *Superparamagnetic iron oxide nanoparticles modified with Tween 80 pass through the intact blood–brain barrier in rats under magnetic field.* ACS applied materials & interfaces, 2016. **8**(18): p. 11336-11341.
85. Sillerud, L.O., et al., *SPION-enhanced magnetic resonance imaging of Alzheimer's disease plaques in AβPP/PS-1 transgenic mouse brain.* Journal of Alzheimer's Disease, 2013. **34**(2): p. 349-365.
86. Chen, Y.-S., et al., *Size-dependent impairment of cognition in mice caused by the injection of gold nanoparticles.* Nanotechnology, 2010. **21**(48): p. 485102.
87. Liu, X., B. Sui, and J. Sun, *Size-and shape-dependent effects of titanium dioxide nanoparticles on the permeabilization of the blood–brain barrier.* Journal of Materials Chemistry B, 2017. **5**(48): p. 9558-9570.
88. Kaushik, A., et al., *Magnetically guided central nervous system delivery and toxicity evaluation of magneto-electric nanocarriers.* Scientific reports, 2016. **6**: p. 25309.
89. Heckman, K.L., et al., *Custom cerium oxide nanoparticles protect against a free radical mediated autoimmune degenerative disease in the brain.* ACS nano, 2013. **7**(12): p. 10582-10596.
90. Portioli, C., et al., *Short-term biodistribution of cerium oxide nanoparticles in mice: Focus on brain parenchyma.* Nanoscience and Nanotechnology Letters, 2013. **5**(11): p. 1174-1181.
91. Shevtsov, M.A., et al., *Recombinant interleukin-1 receptor antagonist conjugated to superparamagnetic iron oxide nanoparticles for theranostic targeting of experimental glioblastoma.* Neoplasia, 2015. **17**(1): p. 32-42.
92. Qiao, R., et al., *Receptor-mediated delivery of magnetic nanoparticles across the blood–brain barrier.* ACS nano, 2012. **6**(4): p. 3304-3310.
93. Yang, J., et al., *Rapid-releasing of HI-6 via brain-targeted mesoporous silica nanoparticles for nerve agent detoxification.* Nanoscale, 2016. **8**(18): p. 9537-9547.
94. Dhakshinamoorthy, V., V. Manickam, and E. Perumal, *Neurobehavioural toxicity of iron oxide nanoparticles in mice.* Neurotoxicity research, 2017. **32**(2): p. 187-203.
95. Xu, L., et al., *Neurotoxicity of silver nanoparticles in rat brain after intragastric exposure.* Journal of nanoscience and nanotechnology, 2015. **15**(6): p. 4215-4223.
96. Vinzant, N., et al., *Iron Oxide Nanoparticle Delivery of Peptides to the Brain: Reversal of Anxiety during Drug Withdrawal.* Frontiers in neuroscience, 2017. **11**: p. 608.
97. Liu, D., et al., *In vitro and in vivo studies on the transport of PEGylated silica nanoparticles across the blood–brain barrier.* ACS applied materials & interfaces, 2014. **6**(3): p. 2131-2136.
98. You, Y., et al., *High- Drug- Loading Mesoporous Silica Nanorods with Reduced Toxicity for Precise Cancer Therapy against Nasopharyngeal Carcinoma.* Advanced Functional Materials, 2017. **27**(42): p. 1703313.
99. Mu, Q., et al., *Gemcitabine and chlorotoxin conjugated iron oxide nanoparticles for glioblastoma therapy.* Journal of Materials Chemistry B, 2016. **4**(1): p. 32-36.
100. Zhao, M., et al., *Develop a novel superparamagnetic nano-carrier for drug delivery to brain glioma.* Drug delivery, 2013. **20**(3-4): p. 95-101.
101. Cheng, K.K., et al., *Curcumin-conjugated magnetic nanoparticles for detecting amyloid plaques in Alzheimer's disease mice using magnetic resonance imaging (MRI).* Biomaterials, 2015. **44**: p. 155-172.
102. Hardas, S.S., et al., *Brain distribution and toxicological evaluation of a systemically delivered engineered nanoscale ceria.* Toxicological sciences, 2010. **116**(2): p. 562-576.

103. Garrido, C., et al., *Gold nanoparticles to improve HIV drug delivery.* Future medicinal chemistry, 2015. **7**(9): p. 1097-1107.
104. Hari, K. and P. Kumpati, *Chitosan tethered colloidal gold nanospheres for drug delivery applications.* Journal of nanoscience and nanotechnology, 2016. **16**(1): p. 229-241.
105. Jampilek, J., et al., *Preparation of silica nanoparticles loaded with nootropics and their in vivo permeation through blood-brain barrier.* BioMed research international, 2015. **2015**.
106. Kiruba Daniel, S., et al., *Synthesis and characterization of fluorophore attached silver nanoparticles.* Bulletin of Materials Science, 2011. **34**(4): p. 639.
107. Dixit, S., et al., *Transferrin receptor-targeted theranostic gold nanoparticles for photosensitizer delivery in brain tumors.* Nanoscale, 2015. **7**(5): p. 1782-1790.
108. Li, C.H., et al., *Gold nanoparticles increase endothelial paracellular permeability by altering components of endothelial tight junctions, and increase blood-brain barrier permeability in mice.* Toxicological Sciences, 2015: p. kfv176.
109. Peng, C., et al., *Targeting orthotopic gliomas with renal-clearable luminescent gold nanoparticles.* Nano Research, 2017. **10**(4): p. 1366-1376.
110. Imam, S.Z., et al., *Iron oxide nanoparticles induce dopaminergic damage: in vitro pathways and in vivo imaging reveals mechanism of neuronal damage.* Molecular neurobiology, 2015. **52**(2): p. 913-926.
111. Wang, J., et al., *Pharmacokinetic parameters and tissue distribution of magnetic Fe3O4 nanoparticles in mice.* International journal of nanomedicine, 2010. **5**: p. 861.
112. Mao, X., et al., *Daunorubicin Loaded Fe3O4 Nanoparticles Induce Apoptosis of Glioma Cells and Disrupt Tight Junction at Blood–Brain Barrier.* Journal of Nanoscience and Nanotechnology, 2016. **16**(12): p. 12356-12361.
113. Nadeem, M., et al., *Uptake and clearance analysis of Technetium99m labelled iron oxide nanoparticles in a rabbit brain.* IET Nanobiotechnology, 2015. **9**(3): p. 136-141.
114. Hu, J., et al., *Asn-Gly-Arg-modified polydopamine-coated nanoparticles for dual-targeting therapy of brain glioma in rats.* Oncotarget, 2016. **7**(45): p. 73681.
115. Guerrero, S., et al., *Improving the brain delivery of gold nanoparticles by conjugation with an amphipathic peptide.* Nanomedicine, 2010. **5**(6): p. 897-913.
116. Kura, A.U., et al., *Acute oral toxicity and biodistribution study of zinc-aluminium-levodopa nanocomposite.* Nanoscale research letters, 2015. **10**(1): p. 105.
117. Dong, E., et al., *Toxicity of nano gamma alumina to neural stem cells.* Journal of nanoscience and nanotechnology, 2011. **11**(9): p. 7848-7856.
118. Huang, N., et al., *Alumina nanoparticles alter rhythmic activities of local interneurons in the antennal lobe of Drosophila.* Nanotoxicology, 2013. **7**(2): p. 212-220.
119. Ali, T., et al., *Anthocyanin-loaded PEG-gold nanoparticles enhanced the neuroprotection of anthocyanins in an Aβ1–42 mouse model of Alzheimer's disease.* Molecular neurobiology, 2017. **54**(8): p. 6490-6506.
120. Disdier, C., et al., *Tissue biodistribution of intravenously administrated titanium dioxide nanoparticles revealed blood-brain barrier clearance and brain inflammation in rat.* Particle and fibre toxicology, 2015. **12**(1): p. 27.
121. Zhao, J., et al., *Influences of nanoparticle zinc oxide on acutely isolated rat hippocampal CA3 pyramidal neurons.* Neurotoxicology, 2009. **30**(2): p. 220-230.
122. Wang, C.-H., et al., *Optimizing the size and surface properties of polyethylene glycol (PEG)–gold nanoparticles by intense x-ray irradiation.* Journal of Physics D: Applied Physics, 2008. **41**(19): p. 195301.
123. Mekawy, M., et al., *Targeting of apoptotic cells using functionalized Fe2O3 nanoparticles.* Nanomaterials, 2015. **5**(2): p. 874-884.
124. Feng, Q., et al., *Self-Assembly of Gold Nanoparticles Shows Microenvironment-Mediated Dynamic Switching and Enhanced Brain Tumor Targeting.* Theranostics, 2017. **7**(7): p. 1875-1889.
125. Wang, P., et al., *Kinetics-mediate fabrication of multi-model bioimaging lanthanide nanoplates with controllable surface roughness for blood brain barrier transportation.* Biomaterials, 2017. **141**: p. 223-232.
126. Zhou, M., et al., *Implications for blood-brain-barrier permeability, in vitro oxidative stress and neurotoxicity potential induced by mesoporous silica nanoparticles: effects of surface modification.* RSC Advances, 2016. **6**(4): p. 2800-2809.

127. Baghirov, H., et al., *Feasibility Study of the Permeability and Uptake of Mesoporous Silica Nanoparticles across the Blood-Brain Barrier.* PLoS One, 2016. **11**(8): p. e0160705.
128. Yin, T., et al., *Penetratin Peptide-Functionalized Gold Nanostars: Enhanced BBB Permeability and NIR Photothermal Treatment of Alzheimer's Disease Using Ultralow Irradiance.* ACS Applied Materials & Interfaces, 2016. **8**(30): p. 19291-19302.
129. Ruan, S., et al., *Tumor microenvironment sensitive doxorubicin delivery and release to glioma using angiopep-2 decorated gold nanoparticles.* Biomaterials, 2015. **37**: p. 425-435.
130. Peiris, P.M., et al., *Treatment of invasive brain tumors using a chain-like nanoparticle.* Cancer research, 2015. **75**(7): p. 1356-1365.
131. You, Y., et al., *Tailored mesoporous silica nanosystem with enhanced permeability of the blood–brain barrier to antagonize glioblastoma.* Journal of Materials Chemistry B, 2016. **4**(36): p. 5980-5990.
132. Ruan, S., et al., *Ligand-Mediated and Enzyme-Directed Precise Targeting and Retention for Enhanced Treatment of Glioblastoma.* ACS Applied Materials & Interfaces, 2017.
133. Hadrup, N., et al., *The similar neurotoxic effects of nanoparticulate and ionic silver in vivo and in vitro.* Neurotoxicology, 2012. **33**(3): p. 416-423.
134. Xu, R., *Progress in nanoparticles characterization: Sizing and zeta potential measurement.* Particuology, 2008. **6**(2): p. 112-115.
135. Zhang, Y., et al., *Zeta potential: a surface electrical characteristic to probe the interaction of nanoparticles with normal and cancer human breast epithelial cells.* Biomedical microdevices, 2008. **10**(2): p. 321-328.
136. Wiley, D.T., et al., *Transcytosis and brain uptake of transferrin-containing nanoparticles by tuning avidity to transferrin receptor.* Proceedings of the National Academy of Sciences, 2013. **110**(21): p. 8662-8667.
137. Sela, H., et al., *Spontaneous penetration of gold nanoparticles through the blood brain barrier (BBB).* Journal of nanobiotechnology, 2015. **13**(1): p. 71.
138. Kouri, F.M., et al., *miR-182 integrates apoptosis, growth, and differentiation programs in glioblastoma.* Genes & development, 2015. **29**(7): p. 732-745.
139. Clark, A.J. and M.E. Davis, *Increased brain uptake of targeted nanoparticles by adding an acid-cleavable linkage between transferrin and the nanoparticle core.* Proceedings of the National Academy of Sciences, 2015. **112**(40): p. 12486-12491.
140. Cabezón, I., et al., *Trafficking of gold nanoparticles coated with the 8D3 anti-transferrin receptor antibody at the mouse blood–brain barrier.* Molecular pharmaceutics, 2015. **12**(11): p. 4137-4145.
141. Kumar, M., et al., *Novel membrane- permeable contrast agent for brain tumor detection by MRI.* Magnetic resonance in medicine, 2010. **63**(3): p. 617-624.
142. Jensen, S.A., et al., *Spherical nucleic acid nanoparticle conjugates as an RNAi-based therapy for glioblastoma.* Science translational medicine, 2013. **5**(209): p. 209ra152-209ra152.
143. Chen, L., B. Zhang, and M. Toborek, *Autophagy is involved in nanoalumina-induced cerebrovascular toxicity.* Nanomedicine: Nanotechnology, Biology and Medicine, 2013. **9**(2): p. 212-221.
144. Bouchoucha, M., et al., *Antibody-conjugated mesoporous silica nanoparticles for brain microvessel endothelial cell targeting.* Journal of Materials Chemistry B, 2017. **5**(37): p. 7721-7735.
145. Li, J., et al., *Comparative study on the acute pulmonary toxicity induced by 3 and 20 nm TiO2 primary particles in mice.* Environmental Toxicology and Pharmacology, 2007. **24**(3): p. 239-244.
146. Sharma, H.S., et al., *Chronic treatment with nanoparticles exacerbate hyperthermia induced blood-brain barrier breakdown, cognitive dysfunction and brain pathology in the rat. Neuroprotective effects of nanowired-antioxidant compound H-290/51.* Journal of nanoscience and nanotechnology, 2009. **9**(8): p. 5073-5090.
147. Sun, C., J.S. Lee, and M. Zhang, *Magnetic nanoparticles in MR imaging and drug delivery.* Advanced drug delivery reviews, 2008. **60**(11): p. 1252-1265.
148. Shukla, A.K., *Emr/esr/epr Spectroscopy for Characterization of Nanomaterials*. 2017: Springer.
149. Ross, F.M., *Opportunities and challenges in liquid cell electron microscopy.* Science, 2015. **350**(6267): p. aaa9886.
150. Liao, H.-G. and H. Zheng, *Liquid cell transmission electron microscopy.* Annual review of physical chemistry, 2016. **67**: p. 719-747.
151. Liang, W.-I., et al., *In Situ Study of Fe3Pt–Fe2O3 Core–Shell Nanoparticle Formation.* Journal of the American Chemical Society, 2015. **137**(47): p. 14850-14853.

152. Zheng, H., et al., *Electron beam manipulation of nanoparticles.* Nano letters, 2012. **12**(11): p. 5644-5648.
153. Gu, M., et al., *Demonstration of an electrochemical liquid cell for operando transmission electron microscopy observation of the lithiation/delithiation behavior of Si nanowire battery anodes.* Nano letters, 2013. **13**(12): p. 6106-6112.
154. Park, J., et al., *Direct observation of nanoparticle superlattice formation by using liquid cell transmission electron microscopy.* Acs Nano, 2012. **6**(3): p. 2078-2085.
155. Klein, K.L., I.M. Anderson, and N. De Jonge, *Transmission electron microscopy with a liquid flow cell.* Journal of microscopy, 2011. **242**(2): p. 117-123.
156. Buchanan, C.F., et al., *Flow shear stress regulates endothelial barrier function and expression of angiogenic factors in a 3D microfluidic tumor vascular model.* Cell adhesion & migration, 2014. **8**(5): p. 517-524.
157. Buchanan, C.F., et al., *Three-dimensional microfluidic collagen hydrogels for investigating flow-mediated tumor-endothelial signaling and vascular organization.* Tissue Engineering Part C: Methods, 2013. **20**(1): p. 64-75.
158. Adriani, G., et al., *A 3D neurovascular microfluidic model consisting of neurons, astrocytes and cerebral endothelial cells as a blood–brain barrier.* Lab on a Chip, 2017. **17**(3): p. 448-459.
159. Brown, J.A., et al., *Recreating blood-brain barrier physiology and structure on chip: A novel neurovascular microfluidic bioreactor.* Biomicrofluidics, 2015. **9**(5): p. 054124.
160. Nørby, P., S. Johnsen, and B.B. Iversen, *In Situ X-ray Diffraction Study of the Formation, Growth, and Phase Transition of Colloidal Cu2–x S Nanocrystals.* ACS nano, 2014. **8**(5): p. 4295-4303.
161. Benfatto, M., et al., *MXAN and Molecular Dynamics: A New Way to Look to the XANES (X-ray Absorption Near Edge Structure) Energy Region,* in *Multiple Scattering Theory for Spectroscopies*. 2018, Springer. p. 197-219.
162. Watkin, S.A., et al., *Microfluidics for Small-Angle X-ray Scattering*, in *X-ray Scattering*. 2017, InTech.
163. Polte, J.r., et al., *Mechanism of gold nanoparticle formation in the classical citrate synthesis method derived from coupled in situ XANES and SAXS evaluation.* Journal of the American Chemical Society, 2010. **132**(4): p. 1296-1301.
164. Polte, J., et al., *Nucleation and growth of gold nanoparticles studied via in situ small angle X-ray scattering at millisecond time resolution.* ACS nano, 2010. **4**(2): p. 1076-1082.
165. Yao, Y., et al., *In situ X-ray absorption spectroscopic study of Fe@ Fe x O y/Pd and Fe@ Fe x O y/Cu nanoparticle catalysts prepared by galvanic exchange reactions.* The Journal of Physical Chemistry C, 2015. **119**(36): p. 21209-21218.
166. Dehouck, M.P., et al., *Drug Transfer Across the Blood‐Brain Barrier: Correlation Between In Vitro and In Vivo Models.* Journal of neurochemistry, 1992. **58**(5): p. 1790-1797.
167. Sharma, H.S., et al., *Influence of engineered nanoparticles from metals on the blood-brain barrier permeability, cerebral blood flow, brain edema and neurotoxicity. An experimental study in the rat and mice using biochemical and morphological approaches.* Journal of nanoscience and nanotechnology, 2009. **9**(8): p. 5055-5072.
168. Sharma, H.S. and A. Sharma, *Neurotoxicity of engineered nanoparticles from metals.* CNS & Neurological Disorders-Drug Targets (Formerly Current Drug Targets-CNS & Neurological Disorders), 2012. **11**(1): p. 65-80.
169. Abbott, N.J., *Blood–brain barrier structure and function and the challenges for CNS drug delivery.* Journal of inherited metabolic disease, 2013. **36**(3): p. 437-449.
170. Fu, T., et al., *Value of functionalized superparamagnetic iron oxide nanoparticles in the diagnosis and treatment of acute temporal lobe epilepsy on MRI.* Neural plasticity, 2016. **2016**.
171. Le Duc, G., et al., *Use of T2‐weighted susceptibility contrast MRI for mapping the blood volume in the glioma‐bearing rat brain.* Magnetic Resonance in Medicine: An Official Journal of the International Society for Magnetic Resonance in Medicine, 1999. **42**(4): p. 754-761.
172. Sharma, A., et al., *Sleep Deprivation-Induced Blood-Brain Barrier Breakdown and Brain Dysfunction are Exacerbated by Size-Related Exposure to Ag and Cu Nanoparticles. Neuroprotective Effects of a 5-HT^ sub 3^ Receptor Antagonist Ondansetron.* Molecular neurobiology, 2015. **52**(2): p. 867.
173. Sharma, A., et al., *Size-and age-dependent neurotoxicity of engineered metal nanoparticles in rats.* Molecular neurobiology, 2013. **48**(2): p. 386-396.

174. Yang, Y.M., et al., *Comparison of USPIO-enhanced MRI and Gd-DTPA enhancement during the subacute stage of focal cerebral ischemia in rats.* Acta Radiologica, 2014. **55**(7): p. 864-873.
175. Shi, J., et al., *An MSN-PEG-IP drug delivery system and IL13Rα2 as targeted therapy for glioma.* Nanoscale, 2017.
176. Aliev, G., et al., *Nanoparticles as alternative strategies for drug delivery to the Alzheimer brain: electron microscopy ultrastructural analysis.* CNS & Neurological Disorders-Drug Targets (Formerly Current Drug Targets-CNS & Neurological Disorders), 2015. **14**(9): p. 1235-1242.
177. André, S., et al., *Validation by magnetic resonance imaging of the diagnostic potential of a heptapeptide-functionalized imaging probe targeted to amyloid-β and able to cross the blood-brain barrier.* Journal of Alzheimer's Disease, 2017. **60**(4): p. 1547-1565.
178. Cabezón, I., et al., *Serial block-face scanning electron microscopy applied to study the trafficking of 8D3-coated gold nanoparticles at the blood–brain barrier.* Histochemistry and cell biology, 2017. **148**(1): p. 3-12.
179. Marinescu, M., et al., *Monitoring therapeutic effects in experimental stroke by serial USPIO-enhanced MRI.* European radiology, 2013. **23**(1): p. 37-47.
180. Wadghiri, Y.Z., et al., *Detection of amyloid plaques targeted by bifunctional USPIO in Alzheimer's disease transgenic mice using magnetic resonance microimaging.* PloS one, 2013. **8**(2): p. e57097.
181. Xie, Y., et al., *Effects of nanoparticle zinc oxide on spatial cognition and synaptic plasticity in mice with depressive-like behaviors.* Journal of biomedical science, 2012. **19**(1): p. 14.
182. Disdier, C., et al., *Brain inflammation, blood brain barrier dysfunction and neuronal synaptophysin decrease after inhalation exposure to titanium dioxide nano-Aerosol in aging rats.* Scientific reports, 2017. **7**(1): p. 12196.
183. Sharma, H.S., et al., *Exacerbation of methamphetamine neurotoxicity in cold and hot environments: neuroprotective effects of an antioxidant compound H-290/51.* Molecular neurobiology, 2015. **52**(2): p. 1023-1033.
184. Sharma, H.S., R. Patnaik, and A. Sharma, *Diabetes aggravates nanoparticles induced breakdown of the blood–brain barrier permeability, brain edema formation, alterations in cerebral blood flow and neuronal injury. An experimental study using physiological and morphological investigations in the rat.* Journal of nanoscience and nanotechnology, 2010. **10**(12): p. 7931-7945.
185. Yang, F., et al., *Minocycline ameliorates hypoxia-induced blood–brain barrier damage by inhibition of HIF-1α through SIRT-3/PHD-2 degradation pathway.* Neuroscience, 2015. **304**: p. 250-259.
186. Ansciaux, E., et al., *In vitro and in vivo characterization of several functionalized ultrasmall particles of iron oxide, vectorized against amyloid plaques and potentially able to cross the blood–brain barrier: toward earlier diagnosis of Alzheimer's disease by molecular imaging.* Contrast media & molecular imaging, 2015. **10**(3): p. 211-224.
187. Maritim, S., et al., *Mapping extracellular pH of gliomas in presence of superparamagnetic nanoparticles: towards imaging the distribution of drug-containing nanoparticles and their curative effect on the tumor microenvironment.* Contrast media & molecular imaging, 2017. **2017**.
188. Fiandra, L., et al., *Nanoformulation of antiretroviral drugs enhances their penetration across the blood brain barrier in mice.* Nanomedicine: Nanotechnology, Biology and Medicine, 2015. **11**(6): p. 1387-1397.
189. Li, Y., et al., *Systematic influence induced by 3 nm titanium dioxide following intratracheal instillation of mice.* Journal of nanoscience and nanotechnology, 2010. **10**(12): p. 8544-8549.
190. Sharma, H.S. and A. Sharma, *Nanowired drug delivery for neuroprotection in central nervous system injuries: modulation by environmental temperature, intoxication of nanoparticles, and comorbidity factors.* Wiley Interdisciplinary Reviews: Nanomedicine and Nanobiotechnology, 2012. **4**(2): p. 184-203.
191. Sharma, H.S. and P.K. Dey, *Probable involvement of 5-hydroxytryptamine in increased permeability of blood-brain barrier under heat stress in young rats.* Neuropharmacology, 1986. **25**(2): p. 161-167.
192. Lowenstein, D.H., R.P. Simon, and F.R. Sharp, *The pattern of 72-kDa heat shock protein-like immunoreactivity in the rat brain following flurothyl-induced status epilepticus.* Brain research, 1990. **531**(1-2): p. 173-182.
193. Wei, L., et al., *Super-multiplex vibrational imaging.* Nature, 2017. **544**(7651): p. 465-470.
194. Bretschneider, S., C. Eggeling, and S.W. Hell, *Breaking the diffraction barrier in fluorescence microscopy by optical shelving.* Physical review letters, 2007. **98**(21): p. 218103.

195. Huang, B., H. Babcock, and X. Zhuang, *Breaking the diffraction barrier: super-resolution imaging of cells.* Cell, 2010. **143**(7): p. 1047-1058.
196. Tsurui, H., et al., *Seven-color fluorescence imaging of tissue samples based on Fourier spectroscopy and singular value decomposition.* Journal of Histochemistry & Cytochemistry, 2000. **48**(5): p. 653-662.
197. Dean, K.M. and A.E. Palmer, *Advances in fluorescence labeling strategies for dynamic cellular imaging.* Nature chemical biology, 2014. **10**(7): p. 512-523.
198. Sitterberg, J., et al., *Utilising atomic force microscopy for the characterisation of nanoscale drug delivery systems.* European Journal of Pharmaceutics and Biopharmaceutics, 2010. **74**(1): p. 2-13.
199. Lamprecht, C., P. Hinterdorfer, and A. Ebner, *Applications of biosensing atomic force microscopy in monitoring drug and nanoparticle delivery.* Expert opinion on drug delivery, 2014. **11**(8): p. 1237-1253.
200. Li, M., et al., *Nanoscale monitoring of drug actions on cell membrane using atomic force microscopy.* Acta Pharmacologica Sinica, 2015. **36**(7): p. 769-782.
201. Lee, S., et al., *Nanoparticle size detection limits by single particle ICP-MS for 40 elements.* Environmental science & technology, 2014. **48**(17): p. 10291-10300.

Highlights

- Metallic-based nanoparticle characterization and in vivo testing is highly varied
- Incomplete characterization complicates understanding in vivo responses
- Widely available techniques for testing should be used to examine nanoparticles
- Standardization could improve nanomedicine comparability, advancing drug delivery

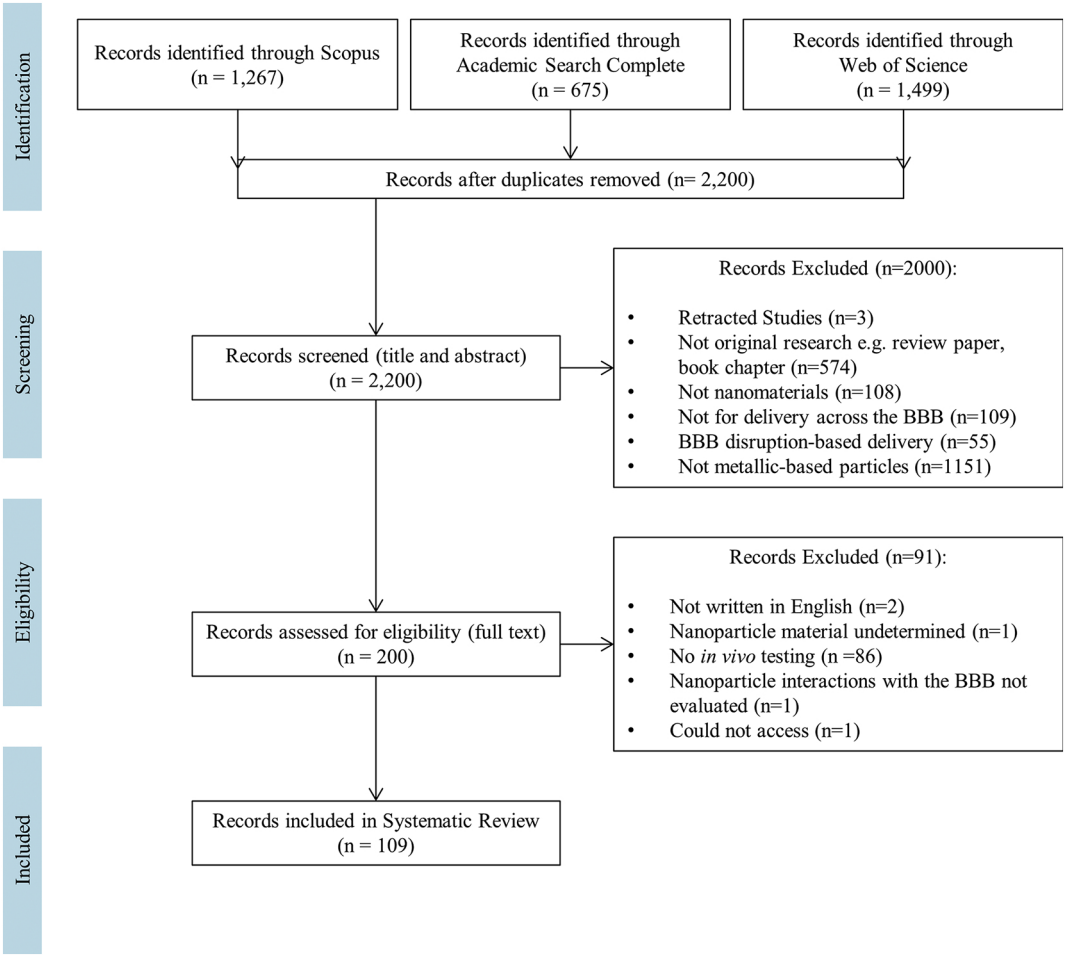
Identification
Screening
Eligibility
Included
Records identified through Scopus (n = 1,267)
Records identified through Academic Search Complete (n = 675)
Records identified through Web of Science (n = 1,499)
Records after duplicates removed (n= 2,200)
Records screened (title and abstract) (n = 2,200)
Records Excluded (n=2000):
Retracted Studies (n=3)
Not original research e.g. review paper, book chapter (n=574)
Not nanomaterials (n=108)
Not for delivery across the BBB (n=109)
BBB disruption-based delivery (n=55)
Not metallic-based particles (n=1151)
Records assessed for eligibility (full text) (n = 200)
Records Excluded (n=91):
Not written in English (n=2)
Nanoparticle material undetermined (n=1)
No *in vivo* testing (n =86)
Nanoparticle interactions with the BBB not evaluated (n=1)
Could not access (n=1)
Records included in Systematic Review (n = 109)

Figure 1

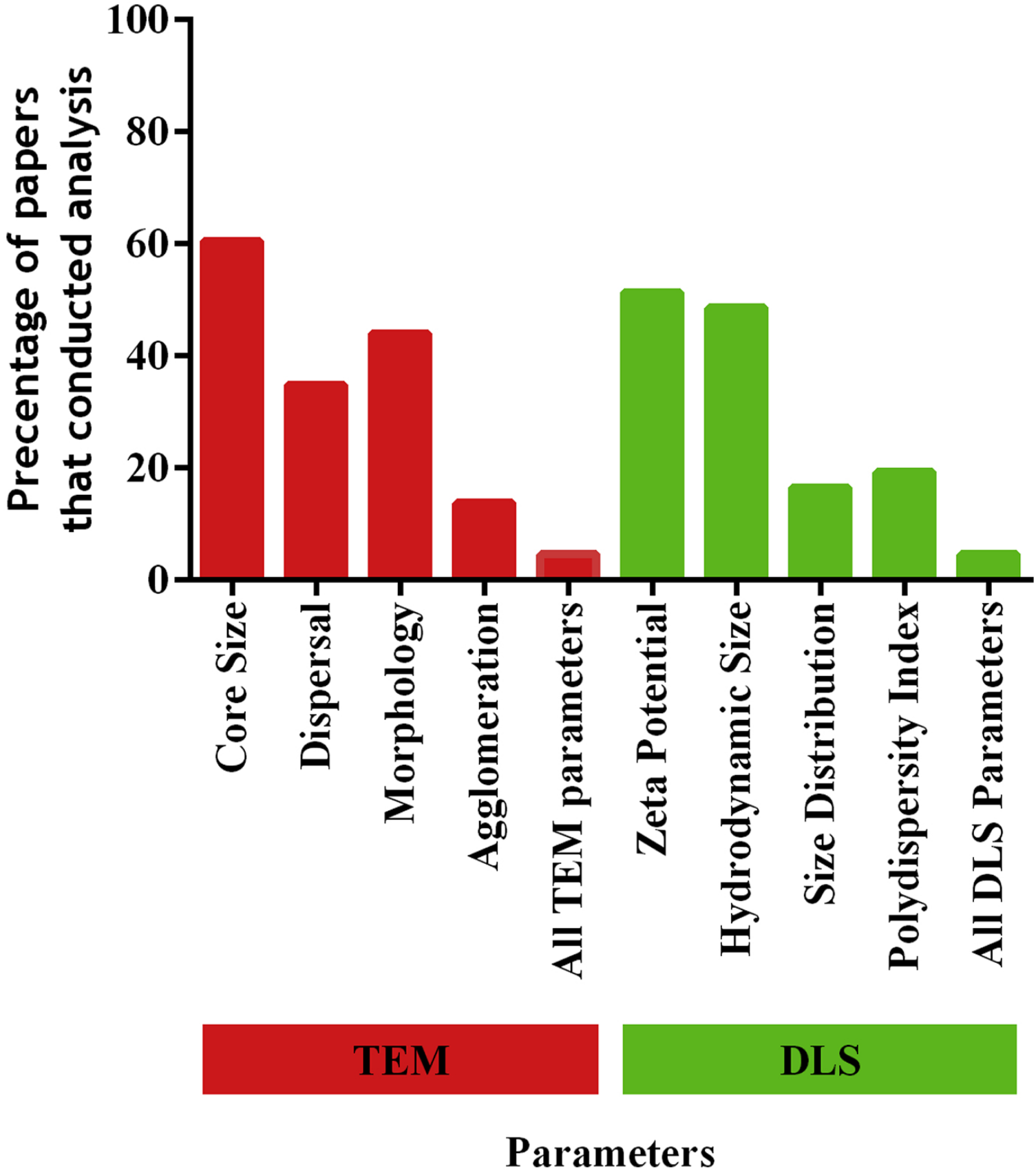
Precentage of papers that conducted analysis
100
80
60
40
20
0
Core Size
Dispersal
Morphology
Agglomeration
All TEM parameters
Zeta Potential
Hydrodynamic Size
Size Distribution
Polydispersity Index
All DLS Parameters
TEM
DLS
Parameters

Figure 2

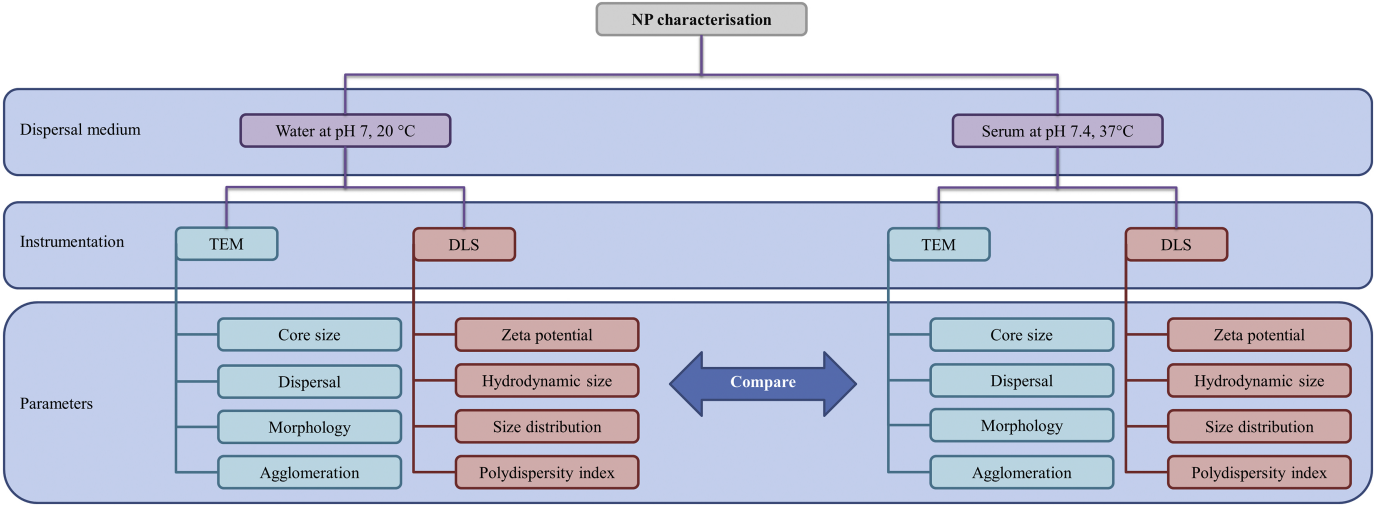
NP characterisation
Dispersal medium
Water at pH 7, 20 °C
Serum at pH 7.4, 37°C
Instrumentation
TEM
DLS
TEM
DLS
Parameters
Core size
Dispersal
Morphology
Agglomeration
Zeta potential
Hydrodynamic size
Size distribution
Polydispersity index
Compare
Core size
Dispersal
Morphology
Agglomeration
Zeta potential
Hydrodynamic size
Size distribution
Polydispersity index

Figure 3

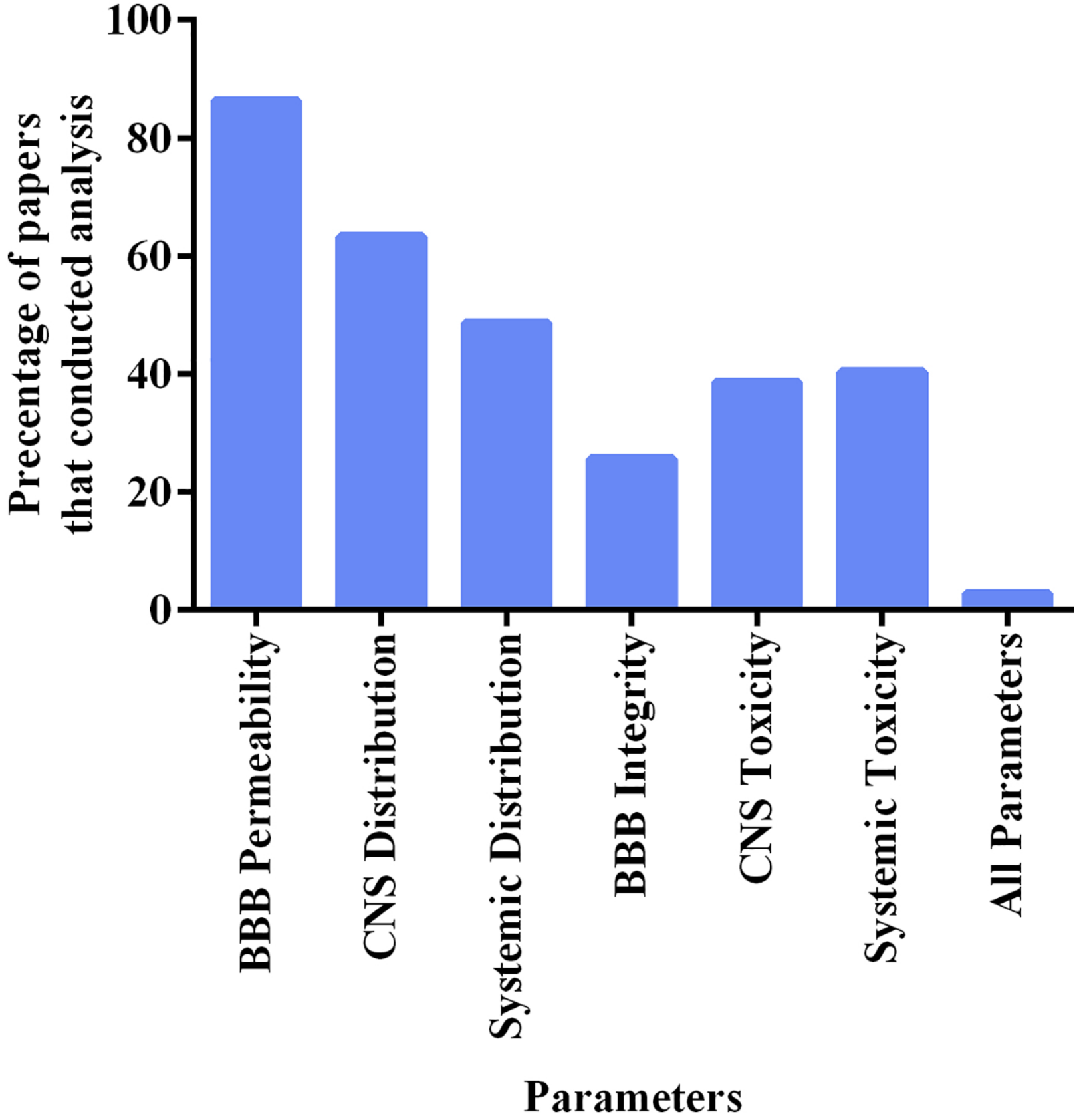
Precentage of papers that conducted analysis
100
80
60
40
20
0
BBB Permeability
CNS Distribution
Systemic Distribution
BBB Integrity
CNS Toxicity
Systemic Toxicity
All Parameters
Parameters

Figure 4

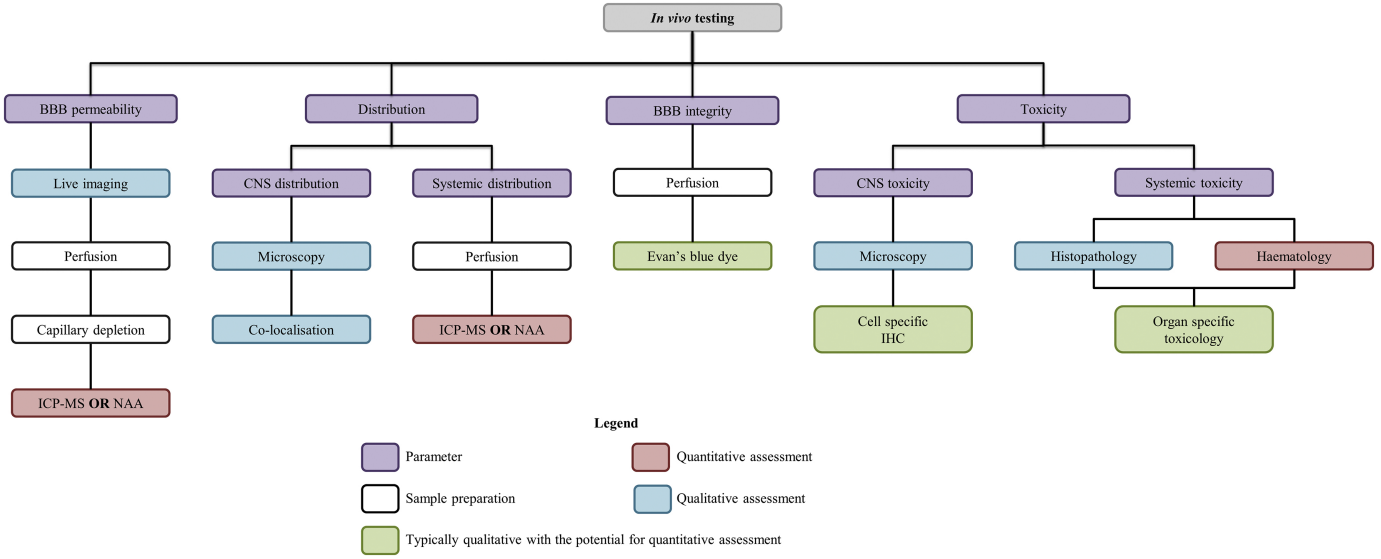
In vivo testing
BBB permeability
Distribution
BBB integrity
Toxicity
Live imaging
CNS distribution
Systemic distribution
Perfusion
CNS toxicity
Systemic toxicity
Perfusion
Microscopy
Perfusion
Evan's blue dye
Microscopy
Histopathology
Haematology
Capillary depletion
Co-localisation
ICP-MS **OR** NAA
Cell specific IHC
Organ specific toxicology
ICP-MS **OR** NAA
Legend
Parameter
Quantitative assessment
Sample preparation
Qualitative assessment
Typically qualitative with the potential for quantitative assessment

Figure 5

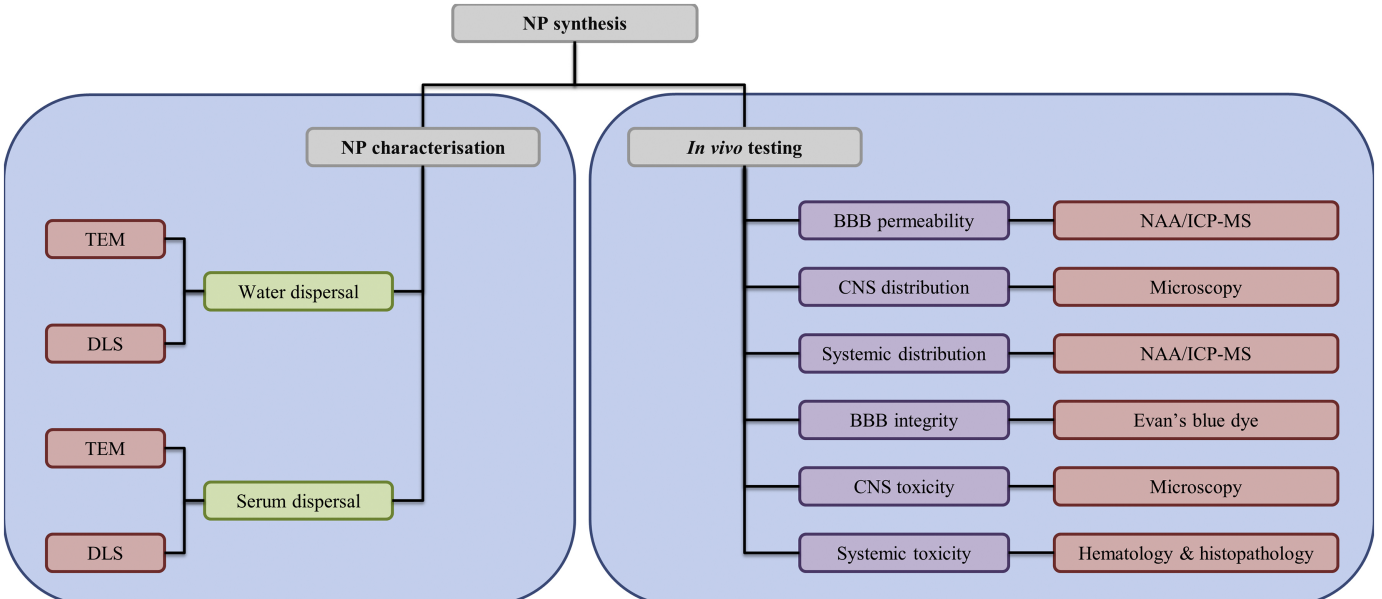
NP synthesis
NP characterisation
TEM
DLS
Water dispersal
TEM
DLS
Serum dispersal
In vivo testing
BBB permeability
NAA/ICP-MS
CNS distribution
Microscopy
Systemic distribution
NAA/ICP-MS
BBB integrity
Evan's blue dye
CNS toxicity
Microscopy
Systemic toxicity
Hematology & histopathology

Figure 6